

UNIVERSITY OF KWAZULU–NATAL

**Exact Solutions in Pure Lovelock Gravity**

Nomfundo Gabuza

**Exact Solutions in Pure Lovelock Gravity by**

**Nomfundo Gabuza**

**Submitted in fulfilment of the  
requirements for the degree of  
Master of Science  
in the  
School of Mathematical Sciences  
University of KwaZulu-Natal**

**As the candidate's supervisor, I have approved this dissertation for submission**

Dr S Hansraj

Name



Signature

22/07/2019

Date

Durban

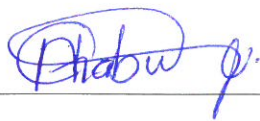
**Dedicated to**

*My late aunt Sis'Thandiwe*

## Preface and Declaration

The research done in this dissertation is original work and has not been previously submitted to any other institution. Where reference to the work of other researchers was made, it has been duly acknowledged.

This thesis was completed under the supervision of Professor S. Hansraj.



Nomfundo Gabuza

## Acknowledgements

I would like to offer my sincere thanks and appreciation to the following people and organisations for their contribution in helping me see this dissertation through to a purposeful end:

- Professor Sudan Hansraj for his guidance, for being an outstanding mentor and for an unreserved support. His expertise in this work has paved a way for my growth as a research scientist. I will forever be grateful to him. I would also like to express my deep appreciation to him for financial assistance throughout the thesis.
- I am grateful to the National Research Foundation (NRF) of South Africa for the award of a masters bursary.
- A special thanks to the University of KwaZulu–Natal for giving me this opportunity to pursue my studies as well as members of staff in the School of Mathematics for the unconditional administrative assistance and encouragement.
- My older sisters Nomonde Gabuza and Nokwanda Gabuza for always keeping me in their prayers.
- Lastly, I am thankful to all my UKZN friends and colleagues for being supportive.

# Abstract

We investigate exact solutions to the odd ( $d = 2N + 1$ ) and even ( $d = 2N + 2$ ) dimensional pure Lovelock field equations in order to generate astrophysical models. New classes of exact solutions are generated by analysing the field equations of pure Gauss–Bonnet gravity ( $N = 2$ ). This is achieved by integrating the pressure isotropy condition with suitable metric potential choices for the critical spacetime dimensions 5 and 6. Amongst the physically important cases we study are the Vaidya–Tikekar superdense star ansatz, the Finch–Skea model as well as isothermal fluids. It is known that in  $5D$  there can exist no bound distribution with a finite radius, while in  $6D$  it was conjectured that all solutions have similar behavior to their  $4D$  counterparts. We consider this with the aid of graphical plots. Lastly we analyse the most general Lovelock polynomials for all  $N$  and  $d$ . We specialise to the cases  $N = 3$ ,  $d = 7$  and  $d = 8$  which has not been considered before in the literature. We analyse the energy density, pressure, energy conditions, sound speed squared, Chandrasekhar adiabatic stability index, compactification ratio and the gravitational mass for models we have discovered. We require these solutions to satisfy conditions for physical admissibility such as a positive pressure and density profile everywhere in the interior of the star and causal behaviour. In addition we examine the Chandrasekhar adiabatic stability criterion to determine whether it is satisfied for dimensions 5, 6 in the Gauss–Bonnet case and third order Lovelock cases since it is expected for 4 dimensions. Classes of exact solutions with pleasing physical behaviour are reported in many cases.

# Contents

<b>1</b>	<b>Introduction</b>	<b>1</b>
<b>2</b>	<b>Mathematical Preliminaries</b>	<b>6</b>
2.1	Introduction . . . . .	6
2.2	Differential Geometry . . . . .	6
2.3	Pure Lovelock gravity . . . . .	10
2.4	Spacetime geometry and field equations . . . . .	11
2.5	Conditions for physical admissibility . . . . .	14
<b>3</b>	<b>Pure Gauss–Bonnet Spacetime of Dimension Five</b>	<b>17</b>
3.1	Introduction . . . . .	17
3.2	Five dimensional field equations . . . . .	18
3.2.1	The Vaidya–Tikekar ansatz . . . . .	20
3.2.2	Interior Schwarzschild solution . . . . .	21
3.2.3	Isothermal fluid: $Z = \text{constant}$ . . . . .	22

3.2.4	Inverse square law fall off with varying potential . . . . .	23
3.2.5	Linear barotropic equation of state . . . . .	25
3.2.6	The Finch–Skea model . . . . .	29
3.2.7	Physical analysis . . . . .	30
3.2.8	Further solvable cases . . . . .	34
3.2.9	Conformal Killing vector . . . . .	38
3.3	Conclusion . . . . .	43
<b>4</b>	<b>Six dimensional Pure Gauss–Bonnet metrics</b>	<b>44</b>
4.1	Introduction . . . . .	44
4.2	Field Equations . . . . .	45
4.2.1	The Vaidya–Tikekar ansatz . . . . .	46
4.2.2	Interior Schwarzschild: $Z = 1 + x$ . . . . .	48
4.2.3	Isothermal fluid: $Z = \text{constant}$ . . . . .	49
4.2.4	Finch–Skea model: $Z = \frac{1}{1+x}$ . . . . .	55
4.2.5	New special cases . . . . .	56
4.2.6	Conformal Killing vector . . . . .	67
4.2.7	Inverse square law for the temporal potential . . . . .	69
4.3	Conclusion . . . . .	70
<b>5</b>	<b>Third Order Lovelock Polynomial</b>	<b>71</b>

5.1	Introduction . . . . .	71
5.2	The general Lovelock case $d = 2N + 1$ . . . . .	72
5.3	The case $d = 2N + 2$ . . . . .	75
5.4	Conclusion . . . . .	77
<b>6</b>	<b>Conclusion</b>	<b>79</b>

# Chapter 1

## Introduction

Gravity is a universal attraction an object produces towards other objects on account of their masses. For centuries Newton's theory of gravity was considered sufficient. However, it failed to explain many observations such as why the perihelion of Mercury was advancing. General Relativity is a leading theory of gravity, proposed by Einstein, built on solid mathematical and physical foundations that explained this and various other behaviours [1]. It is vitally important to the understanding of astrophysical phenomena such as black holes, pulsars, quasars, the final destiny of stars, the big bang, and the universe itself. This theory completely changed our understanding of space-time and gravity. It is often called Einstein's theory of general relativity since Einstein was the one who proposed that gravity is a curvature of space-time geometry instead of a force as in the case of Newtonian theory. A metric theory of gravity requires the construction of a second rank symmetric tensor with vanishing divergence. This may be achieved by varying the action, an invariant quantity constructed from the Riemann curvature, against the metric. In Einstein gravity the variation of the Einstein-Hilbert action with respect to the metric tensor or the trace of the Bianchi identity of the Riemann tensor both generate Einstein's equations [2] [3] [4]. These equations hold the key to our understanding of how

astrophysical distributions behave.

In this work, we focus on a similar theory of gravity but with extra space dimensions, namely Lovelock gravity in higher dimensions. Lovelock theory is a metric theory of gravity yielding conserved second order equations of motion in arbitrary number of dimensions. It generalizes Einstein's general relativity to higher dimensions in a natural way. Lovelock theory coincides with Einstein theory in 3 and 4 dimensions but both theories differ in higher dimensions. Lovelock [5] posed and answered the question: What is the most general tensor theory producing up to second order derivatives in the equations of motion. He proceeded to construct such an action which was quadratic in the Riemann and Ricci tensor as well as the Ricci scalar. The question of the most general scalar-tensor theory yielding second order equations was later answered by Horndeski [6]. Dadhich [7] explains that as Einstein gravity is kinematic in 3 dimensions and becomes dynamic in 4 dimensions, so does Lovelock gravity become kinematic in  $d = 2N + 1$  and dynamic in  $d = 2N + 2$  dimension for any  $N$  [8]. The Lovelock polynomial of order  $N$  regains well known special cases:  $N = 1$  gives the Einstein-Hilbert Lagrangian (linear order) and  $N = 2$  is the Gauss-Bonnet Lagrangian (quadratic) and so on [9]. Since this dissertation focuses largely on  $N = 2$ , the critical spacetime dimensions are  $d = 5, 6$ . Our interest is in using the  $N^{th}$  degree term of Lovelock's polynomial as the generator of the action principle. Therefore we ignore all terms corresponding to lower values of  $N$ .

An exact solution satisfies all the field equations and may be used to develop realistic physical models. They have played a tremendous role in the discussion of physical problems in general relativity. A few examples of these solutions are the Schwarzschild and Kerr [10] solutions for black holes; the Friedmann solutions for cosmology and the plane wave solutions which helped resolve some questions about the existence of gravitational radiation [11]. Exact solutions can help with the

understanding of qualitative features objects might possess. They are also useful in checking the validity of approximation techniques and programs. To say the least, these solutions help us model astrophysical objects and can perform simulations on models to see how they develop in time. This is vitally important since celestial objects take a long time to change state and studying them through observations only is not feasible.

Since our work is dealing with gravity in higher dimensions, it is advisable to begin by considering Einstein–Gauss–Bonnet gravity which goes beyond simply considering higher dimensional general relativity. Gauss–Bonnet gravity is a natural theory of gravity that manifests in the low energy effective action of string theory [12]. It can be described as a generalisation of Einstein gravity which is extended by adding an extra term to the standard Einstein–Hilbert action and is quadratic in the Riemann tensor, Ricci tensor and Ricci scalar. Of course the pure Gauss–Bonnet gravity theory will only consider the  $N = 2$  case solely without the  $N = 0$  (cosmological constant) and  $N = 1$  (Einstein) contributions.

Many researchers have studied Einstein–Gauss–Bonnet theory and found important and interesting results. Hansraj *et al* [13, 14, 15] studied the exact barotropic distributions in Einstein–Gauss–Bonnet gravity and found new exact solutions to the field equations in the Einstein–Gauss–Bonnet modified theory of gravity for a five–dimensional spherically symmetric static distribution of a perfect fluid. They also considered new models for the perfect fluids in Einstein–Gauss–Bonnet gravity. Maeda and Dadhich [16] considered the Kaluza–Klein black hole with negatively curved extra dimensions in string–generated gravity models. They found new exact black hole solutions in Einstein–Gauss–Bonnet gravity with a cosmological constant which bears a specific relation to the Gauss–Bonnet coupling constant.

Einstein–Gauss–Bonnet theory exhibits many pleasing properties since when vary-

ing the extra term with respect to the metric only second order derivatives remain in the field equations and the higher derivative terms cancel out perfectly. As we stated earlier that in dimensions less than or equal to 4, the Gauss–Bonnet gravity and Einstein general relativity are equivalent, and since the Gauss–Bonnet term in the action diminishes to a total derivative and gives a surface integral, it can be said that it does not contribute to Einstein’s equation of motion [17, 18]. It is critical to consider this extra Gauss–Bonnet contribution when dealing with higher dimensions as this extra term is non–trivial when analysing gravity in higher dimensions. If the gravitational action is constructed from cubic curvature invariants, variations are still of the second order and the critical spacetime dimensions are now 7 and 8. More generally, Dadhich [7] asserted that in an  $N$ –dimensional spacetime it is possible to construct an action which is the sum of  $\binom{N+1}{2}$  independent terms which are up to the power of  $\binom{N}{2}$  in the curvature which the variation gives second order field equations for the metric. We emphasise though that in this work our main interest is to isolate the  $N^{\text{th}}$  order term as the action of pure Lovelock gravity.

There is a need for higher dimensional analysis as the Lovelock higher curvature terms only contribute to the dynamics for dimensions higher than 4. The coupling constant itself is dimensionful. As a first step we endeavour to construct models of perfect fluid matter which can be used to model stars. We investigate the behaviour of some well known general relativity models in higher curvature gravity. We probe the Finch–Skea [14, 19] metric ansatz, the Vaidya–Tikekar [20] superdense star model, the interior Schwarzschild solution [21] and the isothermal fluid [22]. We generate their higher curvature counterparts in pure Lovelock gravity and then show the effect of the higher order terms on the gravitational behaviour of perfect fluids.

Our study commences by describing briefly the mathematical context for our work in Chapter 2. In chapter 3 we analyse the field equations of pure Gauss–Bonnet

gravity by using the pure Lovelock equation of odd dimensions. That is, we first set  $N = 2$ ,  $d = 5$  and integrate the pressure isotropy condition to find new exact solutions for the Gauss–Bonnet equations. Next, we make a variety of choices of the spatial metric potential that generate exact solutions. For example the Vaidya–Tikekar prescription, the interior Schwarzschild solution, the isothermal fluid, the Finch–Skea model, the inverse square law fall off of density with varying potential and the linear barotropic equation of state are investigated.

In chapter 4 we study the field equations of pure Gauss–Bonnet gravity for  $d = 2N + 2$ . It is sufficient to set  $N = 2$ ,  $d = 6$  and to integrate the pressure isotropy condition to find exact solutions for the Gauss–Bonnet equations. We examine in detail the Vaidya–Tikekar choice of potential and find new special cases that reduce to hypergeometric functions. Other special cases like the interior Schwarzschild, isothermal fluid and the Finch–Skea model are mentioned but not analysed in detail as this has already been considered elsewhere [23]. Additionally, we analyse the case of the spacetime manifold admitting a one–parameter group of conformal motions, since this is physically reasonable. We further investigate new solutions of the pure Gauss–Bonnet equations which are not related to solutions of Einstein’s equation in  $4D$ .

In chapter 5, we investigate the most general Lovelock polynomial of order  $N$  and  $d$ –dimensions. The critical spacetime dimensions  $d = 2N + 1$  and  $d = 2N + 2$  are considered in general. We consider the cubic case of Lovelock polynomials which has not been studied before in this context. Some new exact solutions are found but a thorough study falls outside the scope of this thesis. Nevertheless, our investigation shows that a rich variety of solutions exist and it is a worthwhile project assessing their viability to represent realistic astrophysical objects.

# Chapter 2

## Mathematical Preliminaries

### 2.1 Introduction

In this chapter we consider some of the main aspects of differential geometry and surface theory which are important to our investigation. We commence by establishing the line element or the metric tensor and then we compute the required Christoffel symbols, Riemann tensor, Ricci tensor, Ricci scalar and Einstein tensor. We also note the Weyl conformal tensor which is useful for checking whether solutions are conformally flat or not.

### 2.2 Differential Geometry

We take spacetime  $M$  to be a 4-dimensional differentiable manifold endowed with a symmetric, nonsingular metric field  $\mathbf{g}$  of signature  $(- + + +)$ . As the metric

tensor field is indefinite the manifold is pseudo-Riemannian. Points in  $M$  are labeled by the real coordinates  $(x^a) = (x^0, x^1, x^2, x^3)$  where  $x^0$  is timelike and  $x^1, x^2, x^3$  are spacelike. The line element is given by

$$ds^2 = g_{ab}dx^a dx^b \quad (2.1)$$

which defines the invariant distance between neighbouring points of a curve in  $M$ . The fundamental theorem of Riemannian geometry guarantees the existence of a unique symmetric connection that preserves inner products under parallel transport. This is called the metric connection  $\Gamma$  or the Christoffel symbol of the second kind. The coefficients of the metric connection  $\Gamma$  are given by

$$\Gamma^a_{bc} = \frac{1}{2}g^{ad}(g_{cd,b} + g_{db,c} - g_{bc,d}) \quad (2.2)$$

where commas denote partial differentiation.

The quantity

$$R^a_{bcd} = \Gamma^a_{bd,c} - \Gamma^a_{bc,d} + \Gamma^a_{ec}\Gamma^e_{bd} - \Gamma^a_{ed}\Gamma^e_{bc} \quad (2.3)$$

is a (1, 3) tensor field and is called the Riemann tensor or the curvature tensor. Upon contraction of the Riemann tensor (2.3) we obtain

$$\begin{aligned} R_{ab} &= R^c_{acb} \\ &= \Gamma^d_{ab,d} - \Gamma^d_{ad,b} + \Gamma^e_{ab}\Gamma^d_{ed} - \Gamma^e_{ad}\Gamma^d_{eb} \end{aligned} \quad (2.4)$$

where  $R_{ab}$  is the Ricci tensor. The Riemann tensor gives an indication of how the metric differs from flatness and the vanishing of this tensor means a flat spacetime.

On contracting the Ricci tensor (2.4) we obtain

$$R = g^{ab}R_{ab}$$

$$= R^a_a \tag{2.5}$$

where  $R$  is the Ricci scalar. The Einstein tensor  $\mathbf{G}$  is constructed in terms of the Ricci tensor (2.4) and the Ricci scalar (2.5) as follows:

$$G^{ab} = R^{ab} - \frac{1}{2}Rg^{ab}. \tag{2.6}$$

The Einstein tensor has zero divergence:

$$G^{ab}{}_{;b} = 0 \tag{2.7}$$

a property referred to in the literature as the contracted Bianchi identity. This identity is useful when studying the conservation of matter which arises as a consequence of the field equations.

An arbitrary rank two tensor can be decomposed into its symmetric and anti-symmetric parts. Similarly the Riemann tensor (2.3) decomposes into the Weyl tensor (or conformal curvature tensor) and parts which involve the Ricci tensor and the curvature scalar. This decomposition is given by

$$\begin{aligned} R_{abcd} &= C_{abcd} - \frac{1}{6}R(g_{ac}g_{bd} - g_{ad}g_{bc}) \\ &+ \frac{1}{2}(g_{ac}R_{bd} - g_{bc}R_{ad} + g_{bd}R_{ac} - g_{ad}R_{bc}) \end{aligned} \tag{2.8}$$

where  $\mathbf{C}$  is the Weyl tensor. The Weyl tensor is trace-free,

$$C^{ab}{}_{ad} = 0$$

and inherits all the symmetry properties of the curvature tensor (2.3). The vanishing of the Weyl tensor is an indication of conformal flatness. This means that the spacetime can be cast into a trivial scaling of the Minkowski spacetime.

The distribution of matter is specified by the energy–momentum tensor  $\mathbf{T}$  which is given by

$$T_{ab} = (\mu + p)u_a u_b + p g_{ab} + q_a u_b + q_b u_a + \pi_{ab} \quad (2.9)$$

for neutral matter. In the above  $\mu$  is the energy density,  $p$  is the isotropic pressure,  $q_a$  is the heat flow vector and  $\pi_{ab}$  represents the stress tensor. These quantities are measured relative to a fluid four–velocity  $\mathbf{u}$  ( $u^a u_a = -1$ ). The heat flow vector and stress tensor satisfy the conditions

$$q^a u_a = 0$$

$$\pi^{ab} u_b = 0$$

In the simpler case of a perfect fluid, which is the case for most cosmological models, the energy–momentum tensor (2.9) has the form

$$T_{ab} = (\mu + p)u_a u_b + p g_{ab}. \quad (2.10)$$

The energy–momentum tensor (2.9) is coupled to the Einstein tensor (2.6) via the Einstein field equations

$$G_{ab} = T_{ab}. \quad (2.11)$$

We utilise normalised units such that the speed of light and the coupling constant are taken to be unity. The field equations (2.11) expresses the relationship of the gravitational field to the matter content. Equation (2.11) is a system of up to ten coupled partial differential equations which are nonlinear and consequently difficult to integrate in general. Here we have provided only a brief outline of the results necessary for later work. For a more detailed exposition of differential geometry applicable to general relativity the reader is referred to de Felice and Clarke (1990), Hawking and Ellis (1973) and Misner *et al* (1973).

## 2.3 Pure Lovelock gravity

The Lovelock polynomial action [5] is given by the Lagrangian

$$\mathcal{L} = \sum_{N=0}^N \alpha_N \mathcal{R}^{(N)} \quad (2.12)$$

where

$$\mathcal{R}^{(N)} = \frac{1}{2^N} \delta_{\alpha_1 \beta_1 \dots \alpha_N \beta_N}^{\mu_1 \nu_1 \dots \mu_N \nu_N} \prod_{r=1}^N R_{\mu_r \nu_r}^{\alpha_r \beta_r} \quad (2.13)$$

and  $\mathcal{R}_{\mu\nu}^{\alpha\beta}$  is  $N$ th order Lovelock analogue of the Riemann tensor as defined in [18].

Also  $\delta_{\alpha_1 \beta_1 \dots \alpha_N \beta_N}^{\mu_1 \nu_1 \dots \mu_N \nu_N} = \frac{1}{N!} \delta_{[\alpha_1}^{\mu_1} \delta_{\beta_1}^{\nu_1} \dots \delta_{\alpha_N}^{\mu_N} \delta_{\beta_N}^{\nu_N]}$  is the generalised Kronecker delta. And where  $\alpha_N$  is a coupling constant which is a number that determines the strength of the force exerted in an interaction. In this case, the Lagrangian of a system is describing an interaction that can be separated into a kinetic part and an interaction part. The coupling constant determines the strength of the interaction part with respect to the kinetic part, or between two sectors of the interaction part.

On variation of the action including the matter Lagrangian with respect to the metric, the equations of motion [18]

$$\sum_{N=0}^N \alpha_N \mathcal{G}_{AB}^{(N)} = \sum_{N=0}^N \alpha_N \left( N \left( \mathcal{R}_{AB}^{(N)} - \frac{1}{2} \mathcal{R}^{(N)} g_{AB} \right) \right) = T_{AB} \quad (2.14)$$

result, where  $\mathcal{R}_{AB}^{(N)} = g^{CD} \mathcal{R}_{ACBD}^{(N)}$ ,  $\mathcal{R}^{(N)} = g^{AB} \mathcal{R}_{AB}^{(N)}$ , and  $T_{AB}$  is the energy momentum tensor. Note that the trace of the Bianchi derivative of the  $N^{th}$  order Riemann tensor,  $\mathcal{R}_{\mu\nu}^{\alpha\beta}$ , gives the corresponding Einstein tensor,  $\mathcal{G}_{AB}^{(N)}$ . This is the gravitational equation in Lovelock gravity which corresponds to the cosmological constant for  $N = 0$ , Einstein equation for  $N = 1$  and to the Gauss–Bonnet equation for  $N = 2$ ,

and so on.

Specialising to the Einstein–Gauss–Bonnet equation we write

$$G_B^A + \alpha H_B^A = T_B^A \quad (2.15)$$

with metric signature  $(- + + + \dots)$  where  $\mathcal{G}_{AB}^{(2)} = H_{AB}$ ,

$$H_{AB} = 2 \left( RR_{AB} - 2R_{AC}R_B^C - 2R^{CD}R_{ACBD} + R_A^{CDE}R_{BCDE} \right) - \frac{1}{2}g_{AB}\mathcal{R}^{(2)}. \quad (2.16)$$

known as the Lanczos tensor [24]

Henceforth we specialize to the pure Lovelock equation involving a single,  $\mathcal{G}_{AB}^{(N)}$ , on the left corresponding to the  $N^{\text{th}}$  term without summing over the lower orders. The equation is then given by

$$\mathcal{G}_{AB}^{(N)} = \left( N \left( \mathcal{R}_{AB}^{(N)} - \frac{1}{2}\mathcal{R}^{(N)}g_{AB} \right) \right) = T_{AB}. \quad (2.17)$$

and these will serve as the master system for our investigation.

## 2.4 Spacetime geometry and field equations

The general static  $d$ –dimensional spherically symmetric metric is taken to be

$$ds^2 = e^\nu dt^2 - e^\lambda dr^2 - r^2 d\Omega_{d-2}^2 \quad (2.18)$$

where  $d\Omega_{n-2}^2$  is the metric on a unit  $(d-2)$ –sphere and where  $\nu = \nu(r)$  and  $\lambda = \lambda(r)$  are the metric potentials. The energy–momentum tensor for the comoving fluid velocity vector  $u^a = e^{-\nu/2}\delta_0^a$  has the form

$$T_b^a = \text{diag}(-\rho, p_r, p_\theta, p_\phi, \dots)$$

for a neutral perfect fluid. Note that in view of spherical symmetry we have for all the  $(d-2)$  angular coordinates  $p_\theta = p_\phi = \dots$ . The conservation laws  $T^{ab}{}_{;b} = 0$  result in the single equation

$$\frac{1}{2} (p_r + \rho) \nu' + p'_r + \frac{(d-2)}{r} (p_r - p_\theta) = 0 \quad (2.19)$$

where primes denote differentiation with respect to  $r$ . This is precisely the same continuity equation in Einstein gravity. Setting  $d = 4$  regains the familiar Einstein case which is called the equation of hydrodynamic equilibrium. This equation may then be written as the Tolman–Oppenheimer–Volkoff equation (TOV) after defining the mass function. The TOV equations have been extensively studied over several decades. The expressions for density, radial and transverse pressure obtained from the pure Lovelock equation are given by

$$\rho = \frac{(d-2)e^{-\lambda} (1 - e^{-\lambda})^{N-1} (rN\lambda' + (d-2N-1)(e^\lambda - 1))}{2r^{2N}} \quad (2.20)$$

$$p_r = \frac{(d-2)e^{-\lambda} (1 - e^{-\lambda})^{N-1} (rN\nu' - (d-2N-1)(e^\lambda - 1))}{2r^{2N}} \quad (2.21)$$

$$\begin{aligned} p_\theta = & \frac{1}{4} r^{-2N} (e^\lambda)^{-N} (e^\lambda - 1)^{N-2} \left[ -Nr\lambda' \left\{ 2(d-2N-1)(e^\lambda - 1) \right. \right. \\ & \left. \left. + r\nu' (e^\lambda - 2N + 1) \right\} + (e^\lambda - 1) \left\{ -2(d-2N-1)(d-2N-2)(e^\lambda - 1) \right. \right. \\ & \left. \left. + 2N(d-2N-1)r\nu' + Nr^2\nu'^2 + 2Nr^2\nu'' \right\} \right] \end{aligned} \quad (2.22)$$

where the Lovelock coupling parameter has been set to unity, without loss of generality, as it is not relevant when considering pure Lovelock gravity.

The equation of pressure isotropy  $p_r = p_\theta$  reads as

$$\begin{aligned} & r\lambda' \left\{ 2(d-2N-1)(e^\lambda - 1) + r\nu' (e^\lambda - 2N + 1) \right\} \\ & - (e^\lambda - 1) \left\{ 4(d-2N-1)(e^\lambda - 1) + r(\nu'(-4N + r\nu' + 2) + 2r\nu'') \right\} = 0 \end{aligned}$$

(2.23)

and will serve as the master differential equation for our study. In what follows we will analyse the pure Gauss–Bonnet equations ( $N = 2$ ) for the critical dimensions 5 and 6, and finally we shall examine the third order pure Lovelock equations ( $N = 3$ ) for spacetime dimensions 7 and 8. Invoking the change of coordinates  $x = Cr^2$ ,  $e^{-\lambda} = Z(x)$  and  $e^\nu = y^2(x)$  we write Eqns (2.20) to (2.22) as

$$\rho = \frac{C^N(d-2)(1-Z)^{N-1} \left[ (d-2N-1)(1-Z) - 2Nx\dot{Z} \right]}{2x^N} \quad (2.24)$$

$$p_r = \frac{C^N(d-2)(1-Z)^{N-1} [4NxZ\dot{y} - (d-2N-1)(1-Z)y]}{2x^N y} \quad (2.25)$$

$$\begin{aligned} p_\theta &= \frac{C^N(1-Z)^{N-2}}{2x^N y} \left[ 8Nx^2Z(1-Z)\ddot{y} \right. \\ &+ 4Nx \left( x(1 + (1-2N)Z)\dot{Z} + (d-2N)Z(1-Z) \right) \dot{y} \\ &\left. + (d-2N-1)(1-Z) \left( 2Nx\dot{Z} - (d-2N-2)(1-Z) \right) y \right] \quad (2.26) \end{aligned}$$

where dots represent differentiation with respect to  $x$ . While the pressure isotropy assumes the form

$$\begin{aligned} 4x^2Z(1-Z)\ddot{y} + \left[ 4(1-N)xZ(1-Z) + 2x^2(1-(2N-1)Z)\dot{Z} \right] \dot{y} \\ + (d-2N-1)(1-Z) \left( \dot{Z}x - Z + 1 \right) y = 0 \quad (2.27) \end{aligned}$$

Note the distinct advantage of the coordinate transformations: equation (2.27) is now a second order linear differential equation in  $y$ . Setting  $N = 1$  yields the standard  $d$ - dimensional equation for Einstein gravity

$$4x^2Z\ddot{y} + 2x^2\dot{Z}\dot{y} + (d-3) \left( \dot{Z}x - Z + 1 \right) y = 0 \quad (2.28)$$

while the pure Gauss–Bonnet equations,  $N = 2$  are given by

$$4x^2 Z(1 - Z)\dot{y} + \left[-4xZ(1 - Z) + 2x^2((1 - 3Z)\dot{Z})\right]\dot{y} \\ + (d - 5)(1 - Z)(\dot{Z}x - Z + 1)y = 0. \quad (2.29)$$

Equation (2.27) may also be arranged as a differential equation in  $Z$  in the form

$$\left[2x^2\dot{y}(2N - 1) + xy(d - 2N - 1)\right]Z\dot{Z} - \left[2x^2\dot{y} + xy(d - 2N - 1)\right]\dot{Z} \\ + [4x(x\dot{y} + \dot{y} - \dot{y}N) - (d - 2N - 1)y]Z^2 \\ - 2[2x(x\dot{y} + \dot{y} - \dot{y}N) - (d - 2N - 1)y]Z - (d - 2N - 1)y = 0 \quad (2.30)$$

but it is now nonlinear in  $Z$ . However (2.30) may also prove useful in finding exact solutions.

## 2.5 Conditions for physical admissibility

We briefly consider some conditions imposed on models to check if they are physically reasonable. We simply extend the familiar conditions of Einstein gravity to check their higher curvature behaviour. Most researchers agree on the following conditions.

- (a) Positivity and finiteness of pressure and energy density everywhere in the interior of the star including the origin and boundary:

$$0 \leq p < \infty \quad 0 < \rho < \infty$$

- (b) The pressure and energy density should be monotonic decreasing functions of the coordinate  $r$ . The pressure vanishes at the boundary  $r = R$  :

$$\frac{dp}{dr} \leq 0 \quad \frac{d\rho}{dr} \leq 0 \quad p(R) = 0$$

(c) Continuity of gravitational potentials across the boundary of the star. The interior line element should be matched smoothly to the generalised exterior Schwarzschild line element at the boundary.

(d) The principle of causality must be satisfied, i.e., the speed of sound should be everywhere less than the speed of light in the interior:

$$0 \leq \frac{dp}{d\rho} \leq 1$$

(e) The metric functions  $e^{2\nu}$  and  $e^{2\lambda}$  should be positive and non-singular everywhere in the interior of the star.

(f) The following energy conditions should be satisfied:

- Weak energy condition:  $\rho - p > 0$
- Strong energy condition:  $\rho + p > 0$
- Dominant energy condition:  $\rho + 3p > 0$

(g) Surface Redshift ( $z = e^{-\lambda} - 1$ ). For static fluid spheres with a monotonically decreasing and positive pressure profile, the surface redshift has been shown to be less than 2. (Buchdahl 1959, Ivanov 2002)

(h) Mass–Radius Ratio: The maximum mass to radius ratio for a static fluid sphere satisfies the condition

$$\frac{\text{mass}}{\text{radius}} < \frac{8}{9}$$

to ensure the stability of the sphere (Buchdahl 1959). We will check whether this still holds for our solutions in higher curvature gravity.

(i) Chandrasekhar adiabatic stability criterion. The quantity  $\left(\frac{\rho+p}{p}\right) \frac{dp}{d\rho}$  is expected to be  $\geq \frac{4}{3}$  [25, 26] for dimension 4. We will check this for the Gauss–Bonnet and third order Lovelock cases.

- (j) The gravitational mass should be an increasing function of the radius.
- (k) The compactification ratio ( $\frac{m}{r}$ ) should be smooth and well behaved in the interior.

Most solutions do not satisfy all the conditions (*a*) to (*k*) throughout the interior of the charged star. Additionally, some of the above conditions may be overly restrictive. For example, observational evidence suggests that in particular stars the energy density  $\rho$  is not a strictly monotonically decreasing function (Shapiro and Teukolsky 1983). The monotonic decrease of density is one important assumption in the proof of Buchdahl's maximum mass–radius ratio. Despite this, it will be interesting to study all of these requirements in the context of higher curvature gravity.

# Chapter 3

## Pure Gauss–Bonnet Spacetime of Dimension Five

### 3.1 Introduction

In this section we will be examining the field equations of pure Gauss–Bonnet gravity using the pure Lovelock equation of odd  $d = 2N + 1$  dimensions. We start by setting up the pure Lovelock equations of motion and setting  $N = 2$  (where  $N$  is the degree of the homogeneous polynomial in the Riemann curvature). Our goal is to integrate the pressure isotropy condition to find exact solutions for the pure Gauss–Bonnet equations. We consider the Finch and Skea solutions on account of its intriguing physical viability as well as acceptability [27]. The solutions of 4 dimensional Einstein gravity suggests that similar solutions to the pure Gauss–Bonnet equations may exist in  $d = 5$ . We additionally study the physical features of the Vaidya–Tikekar ansatz which models superdense stars; the interior Schwarzschild solution; isothermal fluid and other solvable cases. The implications of the existence of a conformal Killing vector are also analysed. Next we evaluate the impact of the inverse square law fall of density with non-constant space potential ( $Z$ ). We use a simple relation

( $p = \omega\rho$ ) which is a barotropic equation of state, where  $\omega$  is the equation of state parameter and  $0 < \omega \leq 1$ . We then generate graphs for appropriate parameter values for the density, pressure, sound speed, gravitational mass, energy conditions and Chandrasekhar adiabatic stability index variables in order to assess the physical viability of our models.

## 3.2 Five dimensional field equations

For  $N = 2$  and  $d = 5$  equation (2.27) assumes the simpler form

$$2xZ(1-Z)\ddot{y} + [2Z(Z-1) + x(1-3Z)\dot{Z}]\dot{y} = 0 \quad (3.1)$$

which is essentially first order linear in  $y$ .

Equation (3.1) may be rearranged in the form

$$\frac{\ddot{y}}{\dot{y}} = \frac{1}{x} - \frac{\dot{Z}}{2} \left[ \frac{2}{Z-1} + \frac{1}{Z} \right] \quad (3.2)$$

and a first integral of (3.2) is

$$\dot{y} = \frac{Ax}{\sqrt{Z}(Z-1)} \quad (3.3)$$

or in general

$$y = A \int \frac{x}{\sqrt{Z}(Z-1)} dx + B \quad (3.4)$$

where  $A$  and  $B$  are constants of integration. From (3.4) we note that once a form for  $Z$  is chosen then a simple integration will yield the form for  $y$  the other potential. An alternative approach is to reconsider equation (3.3). Observe that the result (3.3)

may be arranged as an algebraic equation in  $Z$  and solving for  $Z$  in this equation generates the relationship

$$Z^3 - 2Z^2 + Z - \frac{A^2x^2}{y^2} = 0$$

which has explicit solutions for  $Z$  in terms of  $y$  given by

$$Z_1 = \frac{1}{6} \left( \sqrt[3]{4}W + \frac{\sqrt[3]{16}}{W} + 4 \right) \quad (3.5)$$

$$Z_2 = \frac{1}{12} \left( 2^{2/3}i(\sqrt{3} + i)W - \frac{\sqrt[3]{16}(1 + i\sqrt{3})}{W} + 8 \right) \quad (3.6)$$

$$Z_3 = \frac{1}{12} \left( \frac{\sqrt[3]{16}i(\sqrt{3} + i)}{W} - \sqrt[3]{4}(1 + i\sqrt{3})W + 8 \right) \quad (3.7)$$

where  $W$  is represented by  $W = \sqrt[3]{\frac{27A^2x^2}{y^2} + \sqrt{\frac{27A^2x^2}{y^2} \left( \frac{27A^2x^2}{y^2} - 4 \right)}} - 2$ .

Now it is trivial to choose forms for  $y$  and without performing any integrations we may then determine  $Z$ . We proceed to explore both options (3.4) and (3.5) in what follows. Note that from (3.5 – 3.7) we infer that at least one real-valued function that solves the field equations exists. The expressions for the complex valued functions (3.6) and (3.7) may be discarded as they will not assist in generating stellar models of physical interest.

The energy density and pressure assume the general forms

$$\rho = \frac{6C^2(Z - 1)\dot{Z}}{x} \quad (3.8)$$

$$p = \frac{-12AC^2\sqrt{Z}}{A \int \frac{x}{\sqrt{Z}(Z - 1)} dx + B} \quad (3.9)$$

in terms of the spatial potential  $Z$ .

From (3.9) it can easily be inferred that the pressure may only vanish if  $Z = 0$  (which is inadmissible). This is a known feature of 5 dimensional pure Lovelock gravity that hypersurfaces of vanishing pressure do not exist [23]. In other words no closed compact objects are admitted in 5 dimensional pure Lovelock gravity. Accordingly all perfect fluid solutions must have a cosmological fluid interpretation.

The active gravitational mass formula for five dimensional fluid distributions is given by

$$m = \frac{x(Z-1)\dot{Z}}{2} + K \quad (3.10)$$

with the use of (3.8) and the formula  $m = \int \rho r^{d-2} dr$ , where  $K$  is a constant of integration. The constant  $K$  is set to zero to ensure that  $m(0) = 0$ .

We now consider a variety of choices of the metric potentials that generate exact solutions. These solutions while not representing bounded distributions, may serve to model cosmological fluids. The metric proposals examined below are ones that have historical significance.

### 3.2.1 The Vaidya–Tikekar ansatz

The prescription

$$Z = \frac{1 + ax}{1 + bx} \quad (3.11)$$

generalises that of Vaidya and Tikekar [20]. This choice has proved useful in developing models of superdense stars in standard Einstein theory therefore it is of interest in this modified context.

The general solution of (3.4) is given by

$$y = A \left( \frac{3(a-b)^2 \log \left( 2abx + 2\sqrt{ab(ax+1)(bx+1)} + a+b \right)}{8a^{5/2}\sqrt{b}} + \frac{\sqrt{(ax+1)(bx+1)}(a(2bx+5) - 3b)}{4a^2} \right) + B \quad (3.12)$$

where  $A$  and  $B$  are constants.

We now examine some special cases of importance.

### 3.2.2 Interior Schwarzschild solution

Putting  $b = 0$  and  $a = 1$  in (3.11) gives  $Z = 1 + x$  which corresponds to the Schwarzschild potential. Although this is well known [28], this calculation will help test the veracity of our field equations.

For  $Z = 1 + x$  we find  $y$  to be

$$y = 2A\sqrt{x+1} + B \quad (3.13)$$

as expected. The energy density and pressure are given by

$$\rho = 6C^2 \quad (3.14)$$

$$p = -\frac{12AC^2\sqrt{x+1}}{2A\sqrt{x+1} + B} \quad (3.15)$$

where one of  $A$  or  $B$  should be negative to ensure a positive density and pressure.

The sound speed  $\left(\frac{dp}{d\rho}\right)$  in this case is meaningless as the density is constant. The

expressions relevant to the energy conditions are given by

$$\rho - p = \frac{12AC^2\sqrt{x+1}}{2A\sqrt{x+1}+B} + 6C^2 \quad (3.16)$$

$$\rho + p = 6C^2 - \frac{12AC^2\sqrt{x+1}}{2A\sqrt{x+1}+B} \quad (3.17)$$

$$\rho + 3p = 6C^2 - \frac{36AC^2\sqrt{x+1}}{2A\sqrt{x+1}+B} \quad (3.18)$$

and these should be positive for suitable choices of the integration constants. The mass evaluates to

$$m = \frac{x^2}{2} + K \quad (3.19)$$

where  $K$  is a constant of integration. Setting  $K = 0$ , ensures  $m(0) = 0$ . This case has been well studied by Dadhich et al [23, 28, 29].

### 3.2.3 Isothermal fluid: $Z = \text{constant}$

Isothermal fluids have the property that both energy density and pressure fall off as  $\frac{1}{r^2}$ . It is known that in the standard Einstein theory that a necessary and sufficient condition for isothermal behaviour is a constant gravitational potential  $Z$  [29]. Now for  $Z = \text{a constant}$  we obtain  $\rho = 0$  for the 5 dimensional case and all cases for which  $d = 2N + 1$ . Thus this case is defective.

In all other cases the density behaves as  $\frac{1}{r^2}$ . We shall return to the  $6D$  case later.

### 3.2.4 Inverse square law fall off with varying potential

Let us now consider the prescription of an inverse square law fall of density without

a constant space potential  $Z$ . We set  $\rho = \frac{H}{x}$  (for some constant  $H$ ) in (3.8) to obtain

$$(Z - 1)\dot{Z} = \frac{H}{6C^2} \quad (3.20)$$

and we evaluate  $Z$  as

$$Z = 1 \pm \sqrt{1 + \frac{xH}{3C^2} + A} \quad (3.21)$$

where  $A$  is a constant of integration. The temporal potential assumes the forms

$$y_+ = B - \frac{4A\sqrt{P+3}(4C^2(9A+P+3) - 3Hx)}{15H^2} \quad (3.22)$$

$$y_- = B - \frac{4A\sqrt{3-P}(4C^2(-9A+P-3) + 3Hx)}{15H^2} \quad (3.23)$$

depending on the signature of (3.23). In the above we have put  $P = \sqrt{9A + \frac{3Hx}{C^2} + 9}$

to shorten the lengthy expressions. The energy density and pressure are given by

$$\rho_+ = \frac{H}{x} \quad (3.24)$$

$$\rho_- = \frac{H}{x} \quad (3.25)$$

$$p_+ = \frac{60AH^2\sqrt{P+3}}{4A\sqrt{P+3}(4C^2(9A+P+3) - 3Hx) - 15BH^2} \quad (3.26)$$

$$p_- = \frac{20AH^2(P-3)}{48A^2C^2(P-4) + 32AC^2(P-3) - 4AH(P+1)x - 5BH^2\sqrt{3-P}} \quad (3.27)$$

and the sound speed squared has the form

$$\frac{dp}{d\rho_+} = -x^2 \left( \frac{45AH^3}{C^2P\sqrt{P+3} \left( 4A\sqrt{P+3} (4C^2(9A+P+3) - 3Hx) - 15BH^2 \right)} - \frac{60AH^2\sqrt{P+3} \left( \frac{3AH(4C^2(9A+P+3) - 3Hx)}{C^2P\sqrt{P+3}} + 4A\sqrt{P+3} \left( \frac{6H}{P} - 3H \right) \right)}{\left( 4A\sqrt{P+3} (4C^2(9A+P+3) - 3Hx) - 15BH^2 \right)^2} \right) / H \quad (3.28)$$

$$\frac{dp}{d\rho_-} = -x^2 \left( \frac{30AH^3}{C^2P \left( 48A^2C^2(P-4) + 32AC^2(P-3) - 4AH(P+1)x - 5BH^2\sqrt{3-P} \right)} - \frac{20AH^2(P-3) \left( \frac{72A^2H}{P} - \frac{6AH^2x}{C^2P} - 4AH(P+1) + \frac{48AH}{P} + \frac{15BH^3}{4C^2\sqrt{3-PP}} \right)}{\left( 48A^2C^2(P-4) + 32AC^2(P-3) - 4AH(P+1)x - 5BH^2\sqrt{3-P} \right)^2} \right) / H \quad (3.29)$$

The expressions relevant to the energy conditions for the positive potential are given by

$$(\rho - p)_+ = \frac{H}{x} - \frac{60AH^2\sqrt{P+3}}{4A\sqrt{P+3} (4C^2(9A+P+3) - 3Hx) - 15BH^2} \quad (3.30)$$

$$(\rho + p)_+ = \frac{60AH^2\sqrt{P+3}}{4A\sqrt{P+3} (4C^2(9A+P+3) - 3Hx) - 15BH^2} + \frac{H}{x} \quad (3.31)$$

$$(\rho + 3p)_+ = \frac{180AH^2\sqrt{P+3}}{4A\sqrt{P+3} (4C^2(9A+P+3) - 3Hx) - 15BH^2} + \frac{H}{x} \quad (3.32)$$

The expressions relevant to the energy conditions for negative potential are given by

$$(\rho - p)_- = \frac{H}{x} - \frac{20AH^2(P-3)}{48A^2C^2(P-4) + 32AC^2(P-3) - 4AH(P+1)x - 5BH^2\sqrt{3-P}} \quad (3.33)$$

$$(\rho + p)_- = \frac{20AH^2(P-3)}{48A^2C^2(P-4) + 32AC^2(P-3) - 4AH(P+1)x - 5BH^2\sqrt{3-P}} + \frac{H}{x} \quad (3.34)$$

$$(\rho + 3p)_- = \frac{60AH^2(P - 3)}{48A^2C^2(P - 4) + 32AC^2(P - 3) - 4AH(P + 1)x - 5BH^2\sqrt{3 - P}} + \frac{H}{x} \quad (3.35)$$

The mass evaluates to

$$m = \frac{Hx}{12C^2} + K \quad (3.36)$$

and varies quadratically with the radius. We are electing not to analyse such models in detail as they cannot represent bounded distributions.

### 3.2.5 Linear barotropic equation of state

Assuming a linear dependence of the pressure or the energy density given by  $p = \gamma\rho$  for a real parameter  $\alpha$  constrained by  $0 < \gamma \leq 1$ , we obtain the relationship

$$A \int \frac{x}{\sqrt{Z}(Z - 1)} dx + B = -\frac{2Ax\sqrt{Z}}{\gamma(Z - 1)\dot{Z}} \quad (3.37)$$

Taking the derivative with respect to  $x$  and rearranging the form

$$2Zx(Z - 1)\ddot{Z} + x[(Z + 1) - \gamma(Z - 1)]\dot{Z}^2 - 2Z(Z - 1)\dot{Z} = 0 \quad (3.38)$$

emerges. Equation (3.38) is difficult to solve in general, however, it may be observed that it admits the particular solution  $Z = \text{a constant}$ . This is not a useful solution since in the 5 dimensional case the density vanishes in view of equation (3.8).

We consider some physically important special cases of  $\gamma$ .

- (i).  $\gamma = 1$  (**Stiff fluid**)

This represents an extreme case where the sound speed equals the speed of light. Equation (3.38) simplifies to the form

$$Z(Z-1)[x\ddot{Z} - \dot{Z}] + x\dot{Z}^2 = 0 \quad (3.39)$$

upon rearranging (3.39) and finding the first integral we get the relationship

$$\frac{(Z-1)\dot{Z}}{Z} = x \quad (3.40)$$

or in general

$$Z - \ln Z = \frac{x^2}{2} + A \quad (3.41)$$

where  $A$  is the constant of integration. We have thus established the solution of (3.39) however, it is expressed in implicit form. Since (3.41) is not algebraic, an explicit solution is unlikely. Observe that solution (3.41) is also expressible in terms of the Lambert  $W$  function but this is still not useful in model building.

(ii).  $\gamma = \frac{1}{3}$  (**Incoherent Radiation**)

For the parameter value  $\gamma = \frac{1}{3}$  which corresponds to an incoherent radiating fluid equation (3.38) simplifies to

$$3xZ(Z-1)\ddot{Z} + x(Z+2)\dot{Z}^2 - 3Z(Z-1)\dot{Z} = 0 \quad (3.42)$$

and on rearrangement equation (3.42) may be written in the form

$$\frac{\ddot{Z}}{\dot{Z}} = -\frac{\dot{Z}}{(Z-1)} + \frac{2\dot{Z}}{3Z} + \frac{1}{x}. \quad (3.43)$$

The first integral of (3.43) is

$$\dot{Z} = \frac{AxZ^{\frac{2}{3}}}{(Z-1)} \quad (3.44)$$

where  $A$  is an integration constant.

Equation (3.44) may also be written as

$$\frac{(Z-1)\dot{Z}}{Z^{\frac{2}{3}}} = x \quad (3.45)$$

which has explicit solutions

$$\begin{aligned} Z_1 = & \frac{1}{3} \left( \sqrt{\frac{-12Kx^4 - 24K^2x^2 - 16K^3 + F^{2/3} + 9\sqrt[3]{F} - 2x^6}{\sqrt[3]{F}}} \right. \\ & \left. - \frac{3}{2} \sqrt{-\frac{24}{\sqrt{\frac{-12Kx^4 - 24K^2x^2 - 16K^3 + F^{2/3} + 9\sqrt[3]{F} - 2x^6}{\sqrt[3]{F}}}} + \frac{8(2K+x^2)^3}{9\sqrt[3]{F}} - \frac{1}{9}4\sqrt[3]{F} + 8 + 9} \right) \end{aligned} \quad (3.46)$$

$$\begin{aligned} Z_2 = & \frac{1}{3} \left( \sqrt{\frac{-12Kx^4 - 24K^2x^2 - 16K^3 + F^{2/3} + 9\sqrt[3]{F} - 2x^6}{\sqrt[3]{F}}} \right. \\ & \left. + \frac{3}{2} \sqrt{-\frac{24}{\sqrt{\frac{-12Kx^4 - 24K^2x^2 - 16K^3 + F^{2/3} + 9\sqrt[3]{F} - 2x^6}{\sqrt[3]{F}}}} + \frac{8(2K+x^2)^3}{9\sqrt[3]{F}} - \frac{1}{9}4\sqrt[3]{F} + 8 + 9} \right) \end{aligned} \quad (3.47)$$

$$\begin{aligned} Z_3 = & -\frac{1}{3} \sqrt{\frac{-12Kx^4 - 24K^2x^2 - 16K^3 + F^{2/3} + 9\sqrt[3]{F} - 2x^6}{\sqrt[3]{F}}} \\ & - \frac{1}{2} \sqrt{-\frac{24}{\sqrt{\frac{-12Kx^4 - 24K^2x^2 - 16K^3 + F^{2/3} + 9\sqrt[3]{F} - 2x^6}{\sqrt[3]{F}}}} + \frac{8(2K+x^2)^3}{9\sqrt[3]{F}} - \frac{1}{9}4\sqrt[3]{F} + 8 + 3} \end{aligned} \quad (3.48)$$

$$\begin{aligned}
Z_4 = & -\frac{1}{3} \sqrt{\frac{-12Kx^4 - 24K^2x^2 - 16K^3 + F^{2/3} + 9\sqrt[3]{F} - 2x^6}{\sqrt[3]{F}}} \\
& + \frac{1}{2} \sqrt{\frac{24}{\sqrt{\frac{-12Kx^4 - 24K^2x^2 - 16K^3 + F^{2/3} + 9\sqrt[3]{F} - 2x^6}{\sqrt[3]{F}}}} + \frac{8(2K + x^2)^3}{9\sqrt[3]{F}} - \frac{1}{9}4\sqrt[3]{F} + 8 + 3}
\end{aligned} \tag{3.49}$$

where  $F = -162Kx^4 - 324K^2x^2 + \sqrt{(2K + x^2)^6 (48Kx^4 + 96K^2x^2 + 64K^3 + 8x^6 + 729)} - 216K^3 - 27x^6$  and  $K$  is a constant.

It is interesting that this case gives an explicit solution with equation of state  $p = \frac{1}{3}\rho$  as such solutions are not known in  $4D$  Einstein gravity.

(iii).  $\gamma = -1$  (**Dark Energy**)

In cosmological fluids it is believed that cosmic acceleration is caused by dark energy with equation of state  $p = -\rho$ . In this case equation (3.38) simplifies to

$$x(Z - 1)\ddot{Z} + x\dot{Z}^2 - (Z - 1)\dot{Z} = 0. \tag{3.50}$$

Rearranging and finding the first integral of (3.50) we obtain

$$\dot{Z} = \frac{Ax}{(Z - 1)} \tag{3.51}$$

which has solutions

$$Z = 1 \pm \sqrt{A + 1 + x^2} \tag{3.52}$$

where  $A$  is a constant. The physical consequences of this solution require careful study and this will be done in future work.

### 3.2.6 The Finch–Skea model

Setting  $a = 0$  and  $b = 1$  we get  $Z = \frac{1}{x+1}$ , which is the proposal of Finch and Skea (1989).

The remaining potential evaluates to

$$y = A\sqrt{(1+x)^5} + B \quad (3.53)$$

where  $A$  and  $B$  are constants.

The energy density and pressure are given by

$$\rho = \frac{6C^2}{(x+1)^3} \quad (3.54)$$

$$p = \frac{12AC^2}{A(x+1)^3 - B\sqrt{x+1}} \quad (3.55)$$

while the sound speed squared has the form

$$\frac{dp}{d\rho} = \frac{5A(x+1)^{\frac{7}{2}} \left( 12A(x+1)^{\frac{5}{2}} + 5B \right)}{3 \left( 2A(x+1)^3 + 5B\sqrt{x+1} \right)^2}. \quad (3.56)$$

The expressions that will help us to study the energy conditions are given by

$$\rho - p = \frac{6C^2}{(x+1)^3} - \frac{12AC^2}{A(x+1)^3 - B\sqrt{x+1}} \quad (3.57)$$

$$\rho + p = \frac{12AC^2}{A(x+1)^3 - B\sqrt{x+1}} + \frac{6C^2}{(x+1)^3} \quad (3.58)$$

$$\rho + 3p = \frac{36AC^2}{A(x+1)^3 - B\sqrt{x+1}} + \frac{6C^2}{(x+1)^3} \quad (3.59)$$

The mass evaluates to

$$m = \frac{x^2}{2(x+1)^3} + K \quad (3.60)$$

These results are consistent with the known fact that no pressure free hypersurface is possible in  $5D$  pure Lovelock gravity.

### 3.2.7 Physical analysis

In this section we show that the exact solutions of the Finch–Skea model established in the above section are physically sensible. With the use of the technical computing system Mathematica 11.3 (Wolfram 2018) we create the following plots by making particular parameter choices  $K = 0$ ,  $C = -1$ ,  $A = 1$  with  $B = -0.5$ . Figure 3.1 portrays the behaviour of the energy density versus radial  $r$  coordinate. The energy density is everywhere positive and monotonically decreasing. Figure 3.2 shows the behaviour of pressure versus radial  $r$  coordinate. The pressure is also always positive and approaches zero for large values of the radius. In figure 3.3, this is a negative feature of this model since we expect the sound speed squared to lie between zero and one. In this model causality is violated. Figure 3.4 gives us the relationship between the gravitational mass versus radius. The behaviour of the gravitational mass is reasonable. It is increasing up to a certain radial value and then starts decreasing. The classic behaviour is to have an increasing function. Figure 3.5 shows how the energy conditions behaves against radius. We find that the weak energy condition is violated but the strong and the dominant energy conditions are satisfied. Figure 3.6 gives the behaviour of the Chandrasekhar adiabatic stability index. It is most interesting to find that the Chandrasekhar adiabatic stability index is always  $> \frac{4}{3}$ . This is what is expected for Einstein gravity and it is pleasing to find that there are grounds to believe that it holds also in pure Gauss–Bonnet. Observe also that an irremovable singularity at the centre ( $r = 0$ ) is always present.

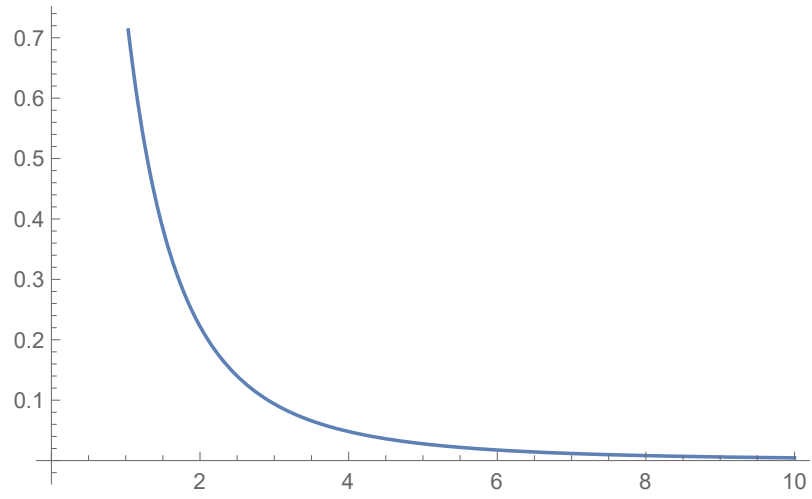


Figure 3.1: Density ( $\rho$ ) versus radius ( $r$ ).

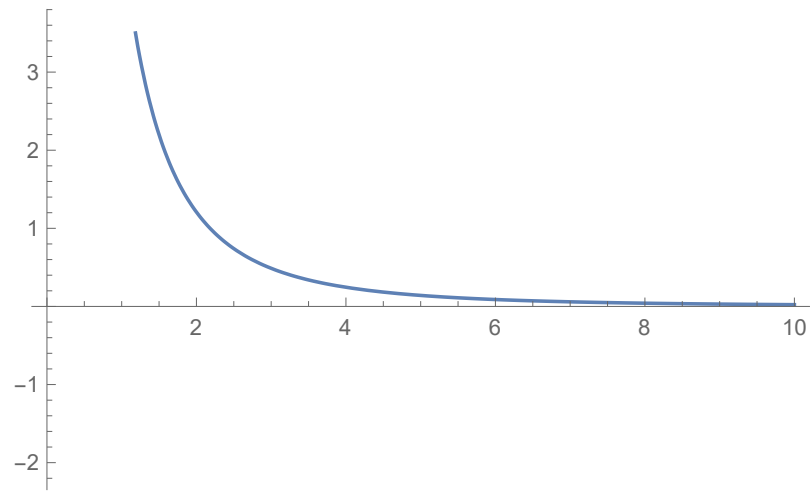


Figure 3.2: Pressure ( $p$ ) versus radius ( $r$ ).

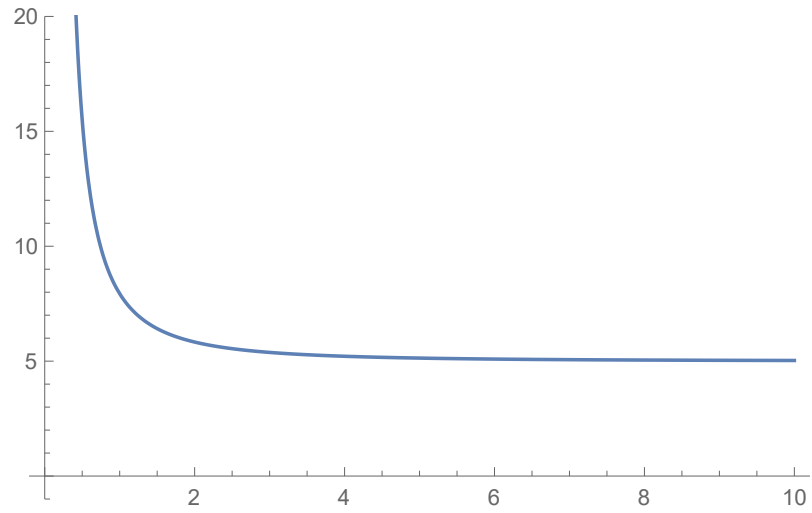


Figure 3.3: Sound speed ( $\frac{dp}{d\rho}$ ) versus radius ( $r$ ).

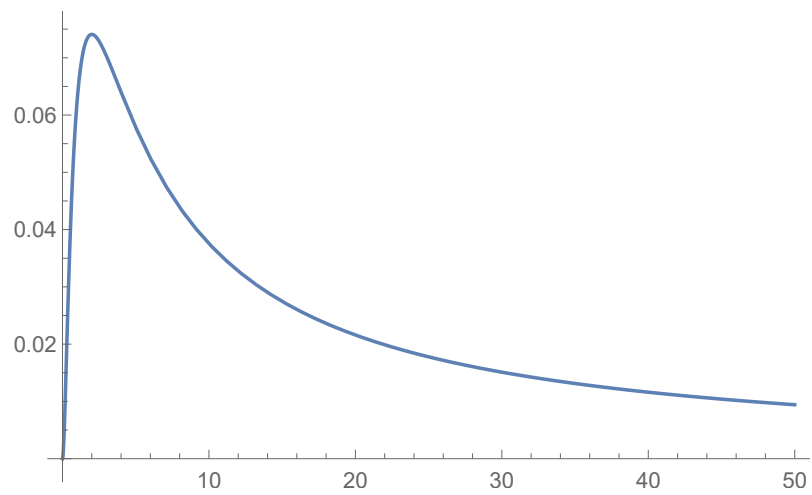


Figure 3.4: Gravitational mass ( $m(r)$ ) versus radius ( $r$ ).

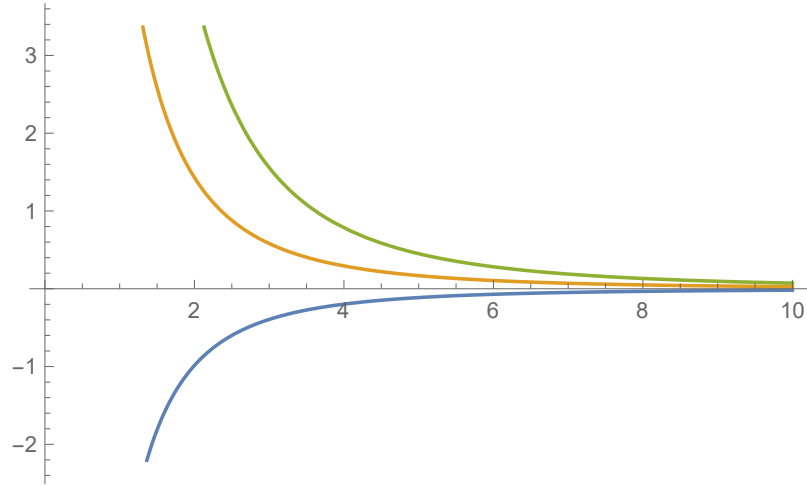


Figure 3.5: Energy conditions  $(\rho - p, \rho + p, \rho + 3p)$  versus radius  $(r)$ .

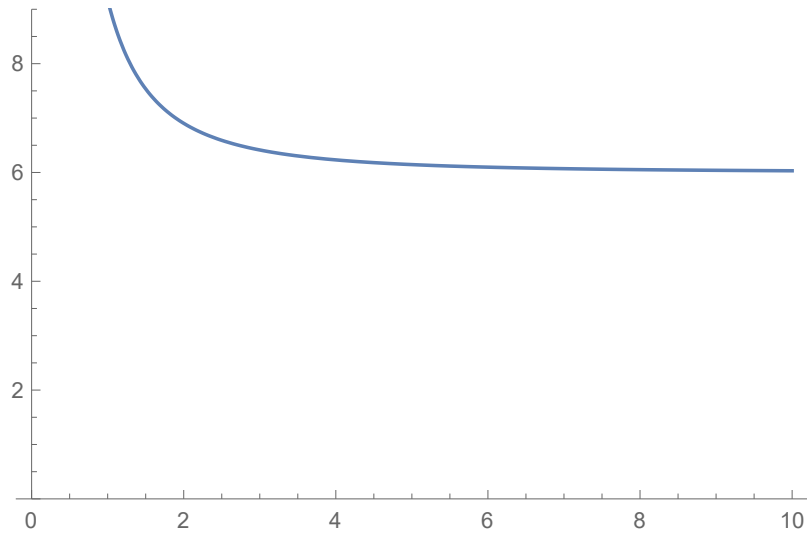


Figure 3.6: Chandrasekhar adiabatic stability index  $\left(\frac{\rho+p}{p}\right) \frac{dp}{d\rho}$  versus radius  $(r)$ .

### 3.2.8 Further solvable cases

In view of our model in (3.2.6) failing to satisfy all the energy conditions, we pursue other options for the metric potentials that give complete models.

For  $Z = x^2 + 1$  we find  $y$  to be

$$y = A \left( \frac{x}{\sqrt{x^2 + 1} + 1} \right) + B \quad (3.61)$$

where  $A$  and  $B$  are constants of integration. Note the absence of any singularities in the metric.

The energy density and pressure are given by

$$\rho = 12C^2 x^2 \quad (3.62)$$

$$p = \frac{12AC^2 \sqrt{x^2 + 1}}{A \log(\sqrt{x^2 + 1} + 1) - A \log(x) - B} \quad (3.63)$$

Note that a simple barotropic equation of state  $p = p(\rho)$  exists in this model. We simply solve for  $x$  in (3.62) and plug into (3.63). This is expected for perfect fluid distributions.

The sound speed has the form

$$\frac{dp}{d\rho} = \frac{A \left( Ax^2 \log(\sqrt{x^2 + 1} + 1) - Ax^2 \log x - Bx^2 + A\sqrt{x^2 + 1} \right)}{2x^2 \sqrt{x^2 + 1} \left( -A \log(\sqrt{x^2 + 1} + 1) + A \log x + B \right)^2} \quad (3.64)$$

The expressions relevant to the energy conditions are given by

$$\rho - p = \frac{12AC^2 \sqrt{x^2 + 1}}{A \log(\sqrt{x^2 + 1} + 1) - A \log(x) - B} + 12C^2 x^2 \quad (3.65)$$

$$\rho + p = 12C^2x^2 + \frac{12AC^2\sqrt{x^2+1}}{A\log(\sqrt{x^2+1}+1) - A\log(x) - B} \quad (3.66)$$

$$\rho + 3p = 12C^2x^2 + \frac{36AC^2\sqrt{x^2+1}}{A\log(\sqrt{x^2+1}+1) - A\log(x) - B} \quad (3.67)$$

The mass is calculated as

$$m = x^4 + K \quad (3.68)$$

where  $K$  is a constant of integration. Setting the parameter values  $K = 0$ ,  $C = 1$ ,  $A = 1$  and  $B = 1$  helps generate the plots of dynamic quantities. These plots show a number of features that satisfy the basic requirements for physical plausibility. Figure 3.7 shows that the energy density ( $\rho$ ) is a positive and a monotonically increasing function. The pressure in Figure 3.8 begins from zero and increases throughout the star. Figure 3.9 portrays a pleasing feature for this model, the behaviour of the sound speed. We observe that the causality principle  $0 \leq \frac{dp}{d\rho} \leq 1$  holds throughout the sphere; this means the sound speed is consistently less than the speed of light. Figure 3.10 shows a monotonically increasing behaviour of the gravitational mass and is positive everywhere as the radius increases. Energy conditions are found to be all positive in figure 3.11. In figure 3.12 we observe a negative feature of this model as we expected the Chandrasekhar adiabatic stability index to be  $> \frac{4}{3}$ .

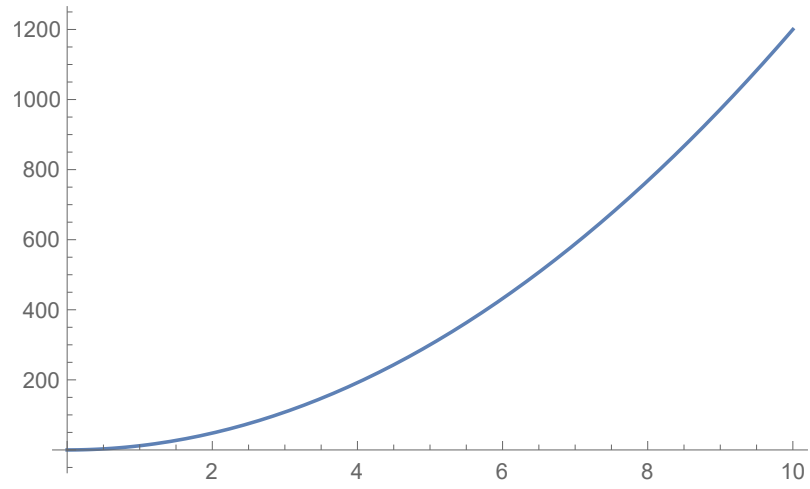


Figure 3.7: Density ( $\rho$ ) versus radius ( $r$ ).

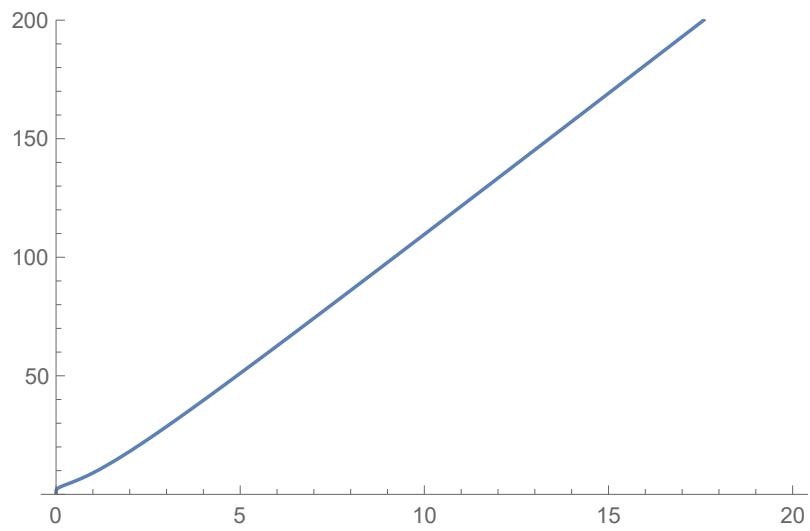


Figure 3.8: Pressure ( $p$ ) versus radius ( $r$ ).

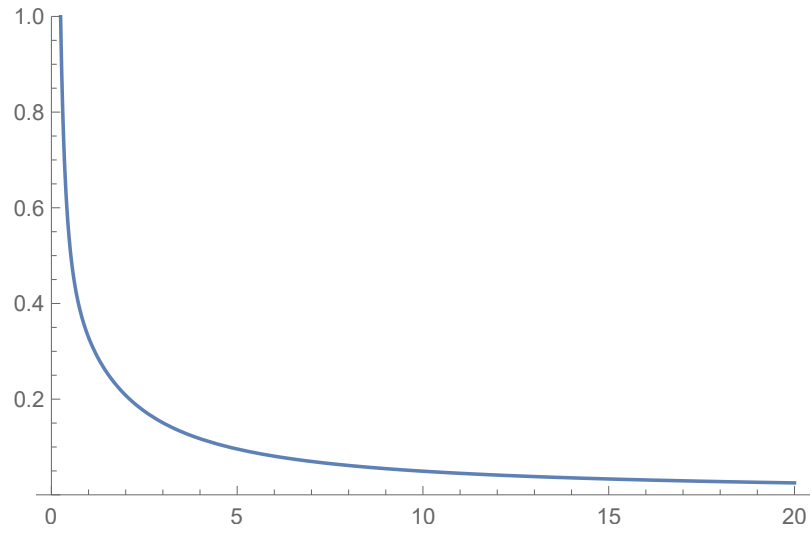


Figure 3.9: Sound speed ( $\frac{dp}{d\rho}$ ) versus radius ( $r$ ).

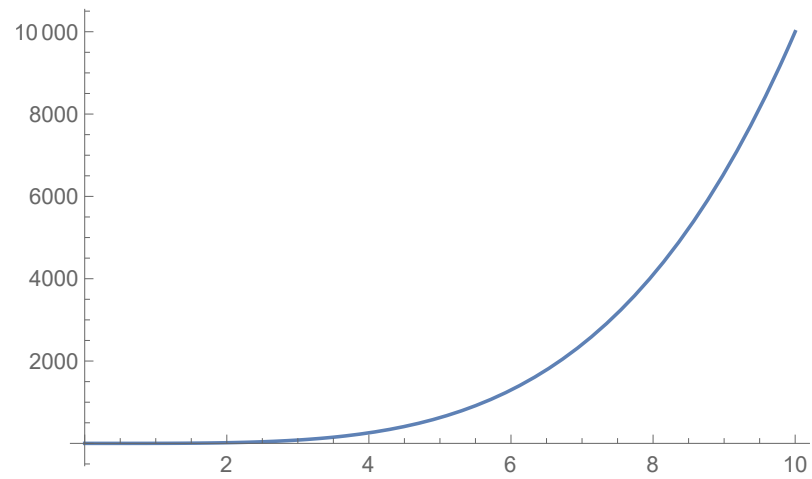


Figure 3.10: Gravitational mass ( $m(r)$ ) versus radius ( $r$ ).

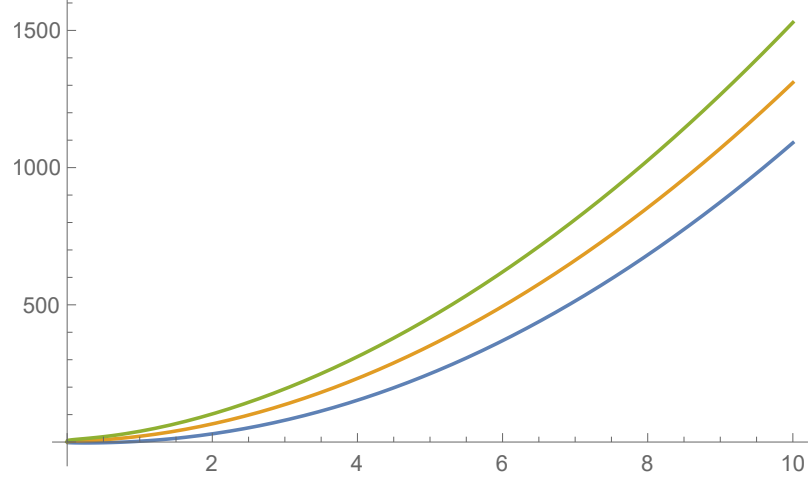


Figure 3.11: Energy conditions  $(\rho - p, \rho + p, \rho + 3p)$  versus radius  $(r)$ .

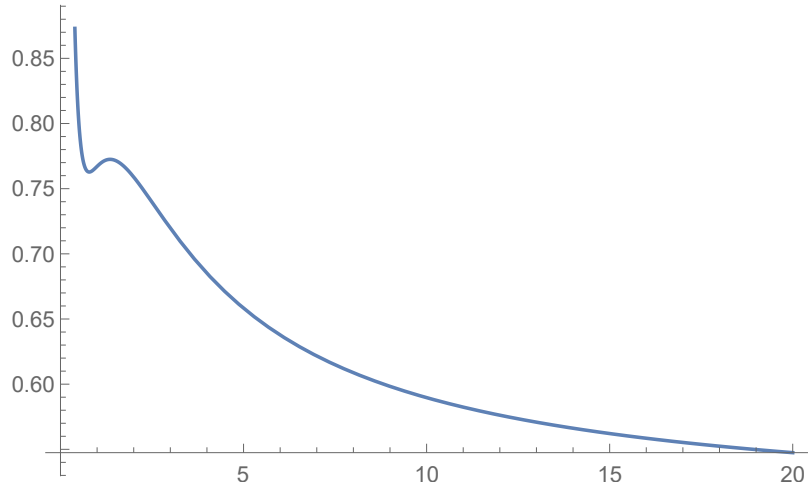


Figure 3.12: Chandrasekhar adiabatic stability index  $\left(\frac{\rho+p}{p}\right) \frac{dp}{d\rho}$  versus radius  $(r)$ .

### 3.2.9 Conformal Killing vector

Changing tactics we now revisit equation (3.5) relating  $Z$  and  $y$ . From the work of Rahman *et al* [30] it is known that for the existence of a conformal Killing vector for our spacetime, a necessary condition is that  $y$  is proportional to  $r^2$ . In our case we

plug in  $y = ax$  in (3.5) to give

$$Z_1 = \frac{1}{6} \left( 2^{2/3} W_1 + \frac{2\sqrt[3]{2}}{W_1} + 4 \right) \quad (3.69)$$

where  $W_1 = \sqrt[3]{\frac{27A^2x^2}{a^2} + \sqrt{\frac{27A^2x^2}{a^4} (27A^2x^2 - 4a^2)}} - 2$ . Note we ignore the complex valued functions as they are not physically important.

The density and pressure are given by

$$\frac{\rho}{C^2} = \frac{1}{x} \left( \frac{1}{6} \left( 2^{2/3} W + \frac{2\sqrt[3]{2}}{W} + 4 \right) - 1 \right) \left( \frac{2^{2/3} S}{3W^2} - \frac{2\sqrt[3]{2} S}{3W^4} \right) \quad (3.70)$$

$$\frac{p}{C^2} = \frac{2}{x^2} \left( 2^{2/3} W_1 + \frac{2\sqrt[3]{2}}{W_1} + 4 \right) \left( \frac{1}{6} \left( -2^{2/3} W_1 - \frac{2\sqrt[3]{2}}{W_1} - 4 \right) + 1 \right) \quad (3.71)$$

where  $S = \frac{54A^2x}{a^2} - \frac{54A^2x \left( 2 - \frac{27A^2x^2}{a^2} \right)}{\sqrt{27A^2x^2(27A^2x^2 - 4a^2)}}$

The mass function has the form

$$m = \frac{x}{12} \left( \frac{1}{6} \left( 2^{2/3} W + \frac{2\sqrt[3]{2}}{W} + 4 \right) - 1 \right) \left( \frac{2^{2/3} S}{3W^2} - \frac{2\sqrt[3]{2} S}{3W^4} \right) \quad (3.72)$$

**Physical Features:** In order to generate plots of the dynamical quantities we choose the parameter values  $K = 0$ ,  $C = 1$ ,  $A = 50$ ,  $a = -1$  and  $B = -1$ . It is clear that in figure 3.13 – 3.14 the energy density and pressure are positive and monotonically decreasing functions throughout the star and approaches zero. In figure 3.15 we observe that the sound speed squared condition behaves as expected since the sound speed lie between zero and one. We observe that in figure 3.16 the weak, strong and dominant energy conditions are satisfied since they are all positive. The weak energy condition is increasing up to a certain radial value and then decreases with the other energy conditions. Figure 3.17 demonstrates the increasing gravitational mass. Figure 3.18 shows the smooth and increasing plot of the compactification

parameter ( $\frac{m}{r}$ ). The Chandrasekhar adiabatic stability index behaviour in figure 3.19 is the pleasing feature for this model. This shows a reasonable behaviour since it is always  $> \frac{4}{3}$  as expected in Einstein gravity and as we promised to check for the pure Gauss–Bonnet.

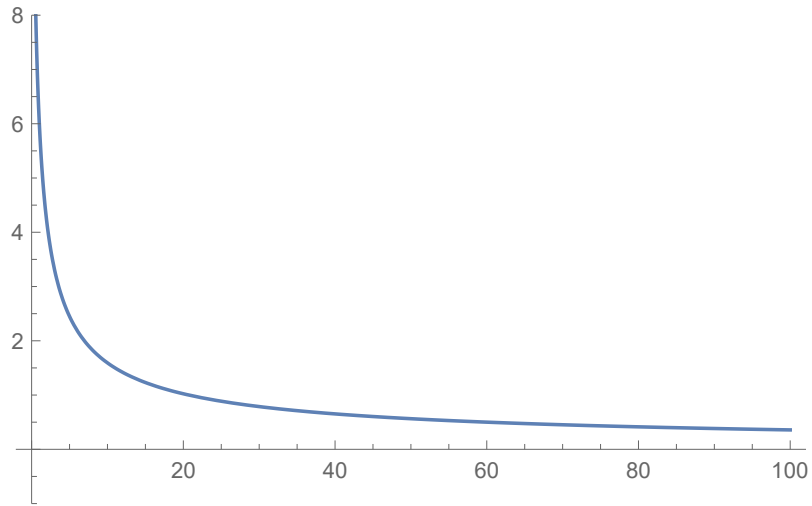


Figure 3.13: Density ( $\rho$ ) versus radius ( $r$ ).

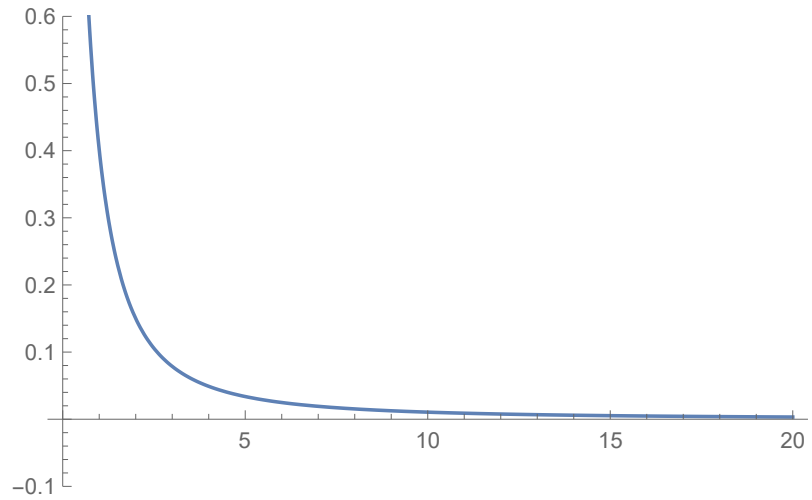


Figure 3.14: Pressure ( $p$ ) versus radius ( $r$ ).

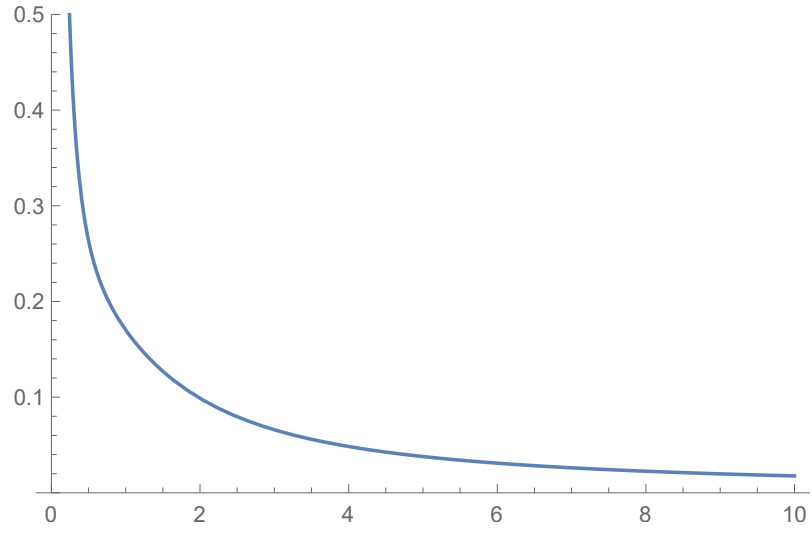


Figure 3.15: Sound speed ( $\frac{dp}{d\rho}$ ) versus radius ( $r$ ).

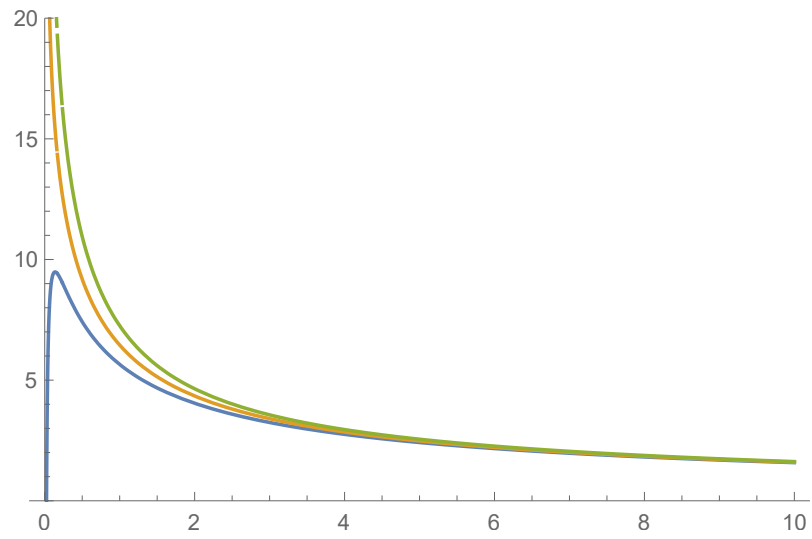


Figure 3.16: Energy conditions ( $\rho - p$ ,  $\rho + p$ ,  $\rho + 3p$ ) versus radius ( $r$ ).

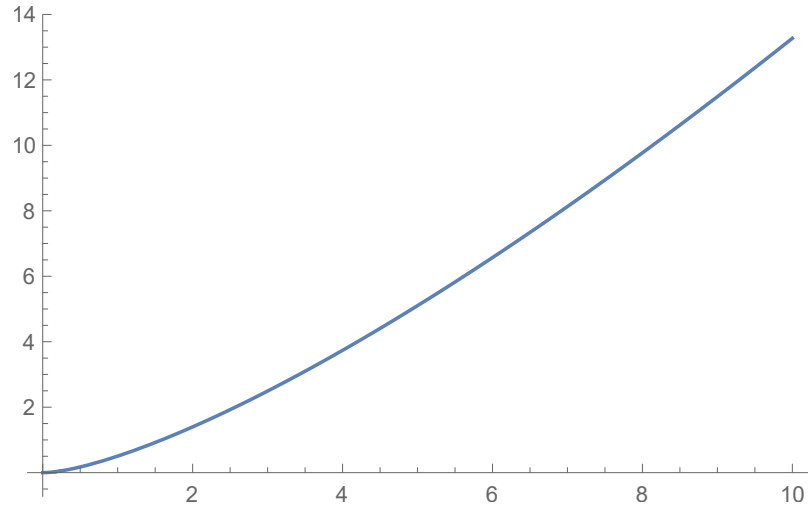


Figure 3.17: Gravitational mass ( $m(r)$ ) versus radius ( $r$ ).

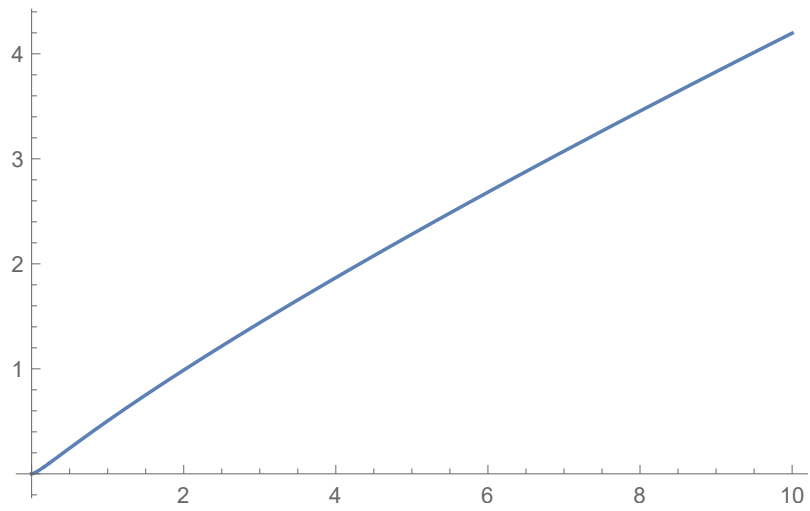


Figure 3.18: Compactification parameter ( $\frac{m}{r}$ ) versus radius ( $r$ ).

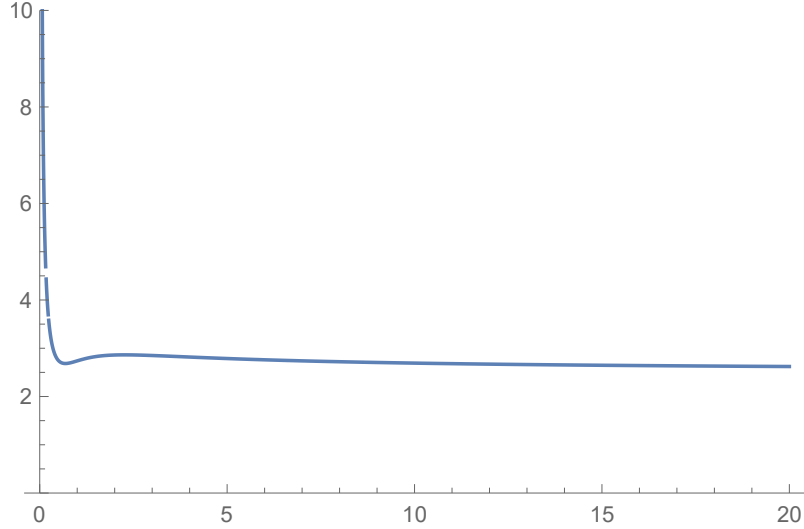


Figure 3.19: Chandrasekhar adiabatic stability index  $\left(\frac{\rho+p}{p}\right) \frac{dp}{d\rho}$  versus radius ( $r$ ).

### 3.3 Conclusion

We examined the field equations of pure Gauss–Bonnet gravity using the pure Lovelock equation of odd  $d = 2N + 1$  dimensions. Exact solutions of the field equations were obtained by intergating the pressure isotropy condition. We analyzed the physical features of the Vaidya–Tikekar ansatz, interior Schwarzschild solution, isothermal fluid and other solvable cases. The implications of the existence of a conformal Killing vector were also analysed. Lastly, the impact of the inverse square law fall of density with non-constant space potential ( $Z$ ) was evaluated and it has been shown that the linear barotropic equation of state exists. In many cases we were able to detect explicit exact solutions, some with violations of one or two of the conditions for physical applicability but at least two of our models satisfied all conditions.

# Chapter 4

## Six dimensional Pure Gauss–Bonnet metrics

### 4.1 Introduction

In the previous chapter we examined the field equations of pure Gauss–Bonnet gravity in odd  $d = 2N + 1$  dimensions. In this chapter, we concentrate on even dimensions ( $d = 2N + 2$ ) and set up the pure Lovelock equations with  $N = 2$ . We proceed to investigate the pressure isotropy condition in order to find exact solutions for the pure Gauss–Bonnet equations of motion. In Einstein gravity Vaidya and Tikekar [20] [31] achieved a solution for a choice of metric ansatz depending on a parameter  $K$ .  $K$  is a measure of deviation from sphericity and indicates a spheroidal geometry in general [31]. A general solution for integer values of  $K$  was obtained by Mukherjee, Paul and Dadhich [21]. It may be noted that this metric ansatz is particularly suited for describing compact objects like neutron stars [32]. The key pressure isotropy equation has an analogous form in  $6D$  to the four dimensional version. Therefore there is the expectation that 4–dimensional solutions could be transformed to higher dimensions with appropriately redefining the parameter  $K$ .

We consider the physical conditions for the general Vaidya–Tikekar solution, and also some special cases like the interior Schwarzschild, isothermal fluids and the Finch-Skea model. Other special cases are also examined. The case of the spacetime manifold admitting a one-parameter group of conformal motions is analysed, as it has physical importance. The study reduces to ordinary differential equations of Abel type. In some cases we obtain exact solutions but in an implicit form. Finally we examine new solutions of the pure Gauss–Bonnet equations which are not necessarily connected to solutions of Einstein’s equation in  $4D$ .

## 4.2 Field Equations

In the  $6D$  case of the pure Gauss–Bonnet equations, the mathematical structure is richer when compared to  $5D$ . For  $N = 2$  and  $d = 6$  equation (2.29) assumes the simpler form

$$4x^2Z(1-Z)\ddot{y} + 2x \left[ x\dot{Z}(1-3Z) - 2Z(1-Z) \right] \dot{y} + (1-Z) \left( x\dot{Z} - Z + 1 \right) y = 0 \quad (4.1)$$

which is a linear second order differential equation in  $y$ . Written in terms of  $Z$  equation (4.1) reads as

$$x(6x\dot{y} + y)Z\dot{Z} - x(2x\dot{y} + y)\dot{Z} + (4x^2\ddot{y} - 4x\dot{y} - y)Z^2 - (4x^2\ddot{y} - 4x\dot{y} - 2y)Z - y = 0 \quad (4.2)$$

and is now nonlinear in  $Z$  but still suitable for finding exact solutions. Unlike the 5 dimensional case it is not possible to separate the gravitational potentials  $Z$  and  $y$ . This means that the detection of exact solutions is a more difficult task.

The equations for energy density, pressure, and mass become

$$\rho = \frac{2C^2(1-Z) [(1-Z) - 4x\dot{Z}]}{x^2} \quad (4.3)$$

$$p = \frac{2C^2(1-Z) [8xZ\dot{y} - (1-Z)y]}{x^2y} \quad (4.4)$$

$$m = \frac{\sqrt{x}(1-Z) [(1-Z) - 4x\dot{Z}]}{10\sqrt{C}} + k \quad (4.5)$$

where  $k$  is a constant of integration. Note we have also used the isotropy equation to eliminate  $\dot{y}$ . Observe immediately that a major and significant deviation from the 5D case is that 6D spacetimes do indeed admit surfaces of vanishing pressure, since it is possible to have  $p(R) = 0$  for a large range of  $Z$  and  $y$  functions. This means that closed hyperspheres of perfect fluids exist for  $D = 6$  in pure Lovelock gravity. Note that the pressure vanishes in general if the potentials behave as

$$y = x^{-\frac{1}{8}} \left( e^{\int \frac{1}{8xz} dx} + c_1 \right) \quad (4.6)$$

for some constant  $c_1$ . Of course this is not desirable. In general, we require a zero pressure for a particular radial value.

We now consider a variety of choices of the metric potentials that generate exact solutions.

### 4.2.1 The Vaidya–Tikekar ansatz

We commence with the choice

$$Z = \frac{1+ax}{1+bx} \quad (4.7)$$

initially made by Buchdahl for the case  $b = 1$  [33] [34]. The proposal (4.7) contains a number of physically important special cases such as the Vaidya–Tikekar [20] superdense stars, the Finch–Skea model [27] as well as the Schwarzschild interior metric. Inserting (4.7) into equation (4.1) generates the differential equation

$$4(ax + 1)(bx + 1)y'' + (-4abx + 2a - 6b)y' + b(b - a)y = 0 \quad (4.8)$$

with the general solution

$$y = \sqrt[4]{\frac{b^3}{a}} \left( A {}_2F_1 \left( -\frac{2a + \sqrt{a(5a - b)}}{2a}, \frac{\sqrt{a(5a - b)}}{2a} - 1; \frac{1}{2}; -\frac{axb + b}{a - b} \right) + B \sqrt{\frac{abx + b}{a - b}} {}_2F_1 \left( \frac{\sqrt{a(5a - b)} - a}{2a}, -\frac{a + \sqrt{a(5a - b)}}{2a}; \frac{3}{2}; -\frac{axb + b}{a - b} \right) \right) \quad (4.9)$$

where  $A, B$  are constants and  ${}_2F_1$  is the well known hypergeometric function.

The solution in terms of hypergeometric functions is not useful in the process of modelling. However it is known that hypergeometric functions reduce to elementary functions in certain cases. We try to find such special cases.

On analysing the general solution (4.9) we observe that several new classes of solutions in terms of elementary functions are possible. The analysis rests on finding integral solutions to the algebraic equation

$$5a^2 - ab = c^2$$

for  $a, b, c$  integers in order to nullify the square roots so that elementary functions result. Clearly there are an infinite number of solutions, however, for a chosen  $c$  only a few cases exist for  $a$  and  $b$ . We present a table showing some possible integral solutions for  $a$  and  $b$  for each choice of  $c$ . We omit the trivial case  $a = b$ .

$c$	$\{(a ; b)\}$
0	$\infty, \{(a ; 5a)\}$
1	$(-1 ; -4), (1 ; 4)$
4	$(-4 ; -19), (-2 ; -8), (2 ; 8), (4 ; 19)$
9	$(-9 ; -44), (-3 ; -12), (-1 ; 4), (1 ; -4), (3 ; 12), (9 ; 44)$
16	$(-16 ; -79), (-8 ; -38), (-4 ; -16), (-1 ; 11), (1 ; -11), (4 ; 16), (8 ; 38), (16 ; 79)$

Table 4.1: Table showing possible integral solutions for  $a$  and  $b$  for each choice of  $c$ .

Note also that other generic classes of solutions exist such as  $b = \pm 4a$ ,  $b = -20a$ ,  $b = -44a$  etc. Therefore the hypergeometric function in this problem gives large classes of exact solutions in elementary functions. However we elect to study exact models that are potentially physically reasonable.

#### 4.2.2 Interior Schwarzschild: $Z = 1 + x$

Setting  $b = 0$  and  $a = 1$  gives  $Z = 1 + x$ , we obtain by integration

$$y = 2A\sqrt{x+1} + B \quad (4.10)$$

which is the space potential for the Schwarzschild metric in any spacetime dimension [15]. It is independent of spacetime dimension  $d$  and the order of the Lovelock polynomial  $N$  [23].

The energy density and pressure are given by

$$\rho = 10C^2 \quad (4.11)$$

$$p = -\frac{2C^2 \left( 10A\sqrt{x+1} + B \right)}{2A\sqrt{x+1} + B} \quad (4.12)$$

as anticipated. The expressions relevant to the energy conditions have the form

$$\rho - p = \frac{2C^2 (10A\sqrt{x+1} + B)}{2A\sqrt{x+1} + B} + 10C^2 \quad (4.13)$$

$$\rho + p = 10C^2 - \frac{2C^2 (10A\sqrt{x+1} + B)}{2A\sqrt{x+1} + B} \quad (4.14)$$

$$\rho + 3p = 10C^2 - \frac{6C^2 (10A\sqrt{x+1} + B)}{2A\sqrt{x+1} + B} \quad (4.15)$$

while the mass evaluates to

$$m = \frac{1}{2} \sqrt{\frac{x^5}{C}} + K \quad (4.16)$$

where  $K$  is a constant of integration. These expressions conform to our expectations. There is no need to study them in detail as this is already known.

### 4.2.3 Isothermal fluid: $Z = \text{constant}$

In Einstein theory it is known that a constant metric potential  $Z$  gives isothermal behaviour [23]. For  $Z = k$  we find  $y$  to be

$$y = x^{1-\frac{1}{2}\sqrt{\frac{5k-1}{k}}} \left( A + Bx\sqrt{\frac{5k-1}{k}} \right) \quad (4.17)$$

where  $A$  and  $B$  are constants of integration. The energy density and pressure are given by

$$\rho = \frac{2C^2(k-1)^2}{x^2} \quad (4.18)$$

$$p = -\frac{2C^2\sqrt{k-1} \left( Ba_1x\sqrt{\frac{5k-1}{k}} + Aa_2 \right)}{x^2 \left( Bx\sqrt{\frac{5k-1}{k}} + A \right)} \quad (4.19)$$

where we have put  $a_1 = \sqrt{k-1}(9k-1) - 4\sqrt{k(1-k)(1-5k)}$  and  $a_2 = \sqrt{k-1}(9k-1) + 4\sqrt{k(1-k)(1-5k)}$  to simplify the expressions. Note that a surface of vanishing pressure ( $p = 0$ ) exists for  $x = \left(-\frac{Aa_2}{Ba_1}\right)\sqrt{\frac{k}{1-5k}}$ . Isothermal behaviour results when  $A = 0$ . ( $p \sim \frac{1}{r^2}; \rho \sim \frac{1}{r^2}$ ) but not otherwise. We consider the most general  $A \neq 0$  case.

The sound speed squared has the form

$$\begin{aligned} \frac{dp}{d\rho} = & -x^3 \left( \frac{2\sqrt{1-k}\sqrt{1-5k} \left( a_1 x \sqrt{\frac{5k-1}{k}} + a_2 \sqrt{1-5k} \right) x^{\frac{\sqrt{5k-1}}{\sqrt{k}}-3}}{\sqrt{k} \left( x \sqrt{\frac{5k-1}{k}} + 1 \right)^2} \right. \\ & - \left. \frac{2\sqrt{1-5k}\sqrt{1-k} a_1 x^{\frac{\sqrt{5k-1}}{\sqrt{k}}-3}}{\sqrt{k} \left( x \sqrt{\frac{5k-1}{k}} + 1 \right)} + \frac{4\sqrt{k-1} \left( a_1 x \sqrt{\frac{5k-1}{k}} + a_2 \right)}{x^3 \left( x \sqrt{\frac{5k-1}{k}} + 1 \right)} \right) \\ & / (4(k-1)^2) \end{aligned} \quad (4.20)$$

The expressions needed to study the energy conditions are expressed as

$$\rho - p = \frac{2C^2(k-1)^2}{x^2} + \frac{2C^2\sqrt{k-1} \left( Ba_1 x \sqrt{\frac{5k-1}{k}} + Aa_2 \right)}{x^2 \left( Bx \sqrt{\frac{5k-1}{k}} + A \right)} \quad (4.21)$$

$$\rho + p = \frac{2C^2(k-1)^2}{x^2} - \frac{2C^2\sqrt{k-1} \left( Ba_1 x \sqrt{\frac{5k-1}{k}} + Aa_2 \right)}{x^2 \left( Bx \sqrt{\frac{5k-1}{k}} + A \right)} \quad (4.22)$$

$$\rho + 3p = \frac{2C^2(k-1)^2}{x^2} - \frac{6C^2\sqrt{k-1} \left( Ba_1 x \sqrt{\frac{5k-1}{k}} + Aa_2 \right)}{x^2 \left( Bx \sqrt{\frac{5k-1}{k}} + A \right)} \quad (4.23)$$

while in the  $6D$  case the mass has the simple form

$$m = \frac{\sqrt{x}(k-1)^2}{10\sqrt{C}} + K \quad (4.24)$$

where  $K$  is a constant of integration.

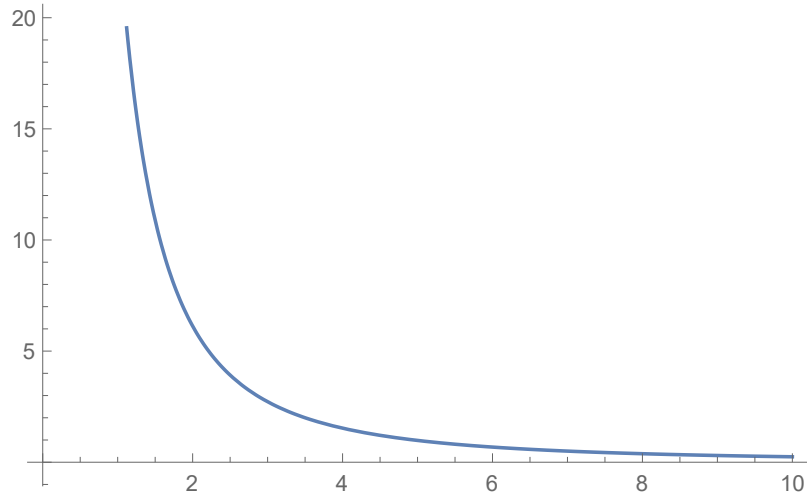


Figure 4.1: Density ( $\rho$ ) versus radius ( $r$ ).

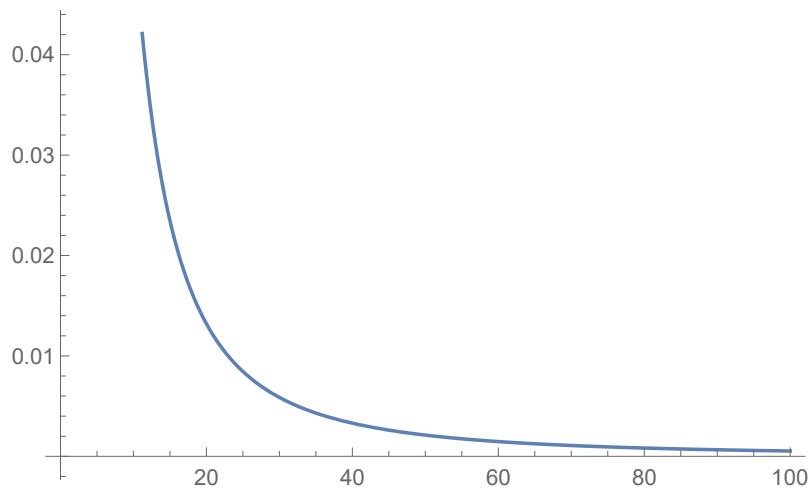


Figure 4.2: Pressure ( $p$ ) versus radius ( $r$ ).

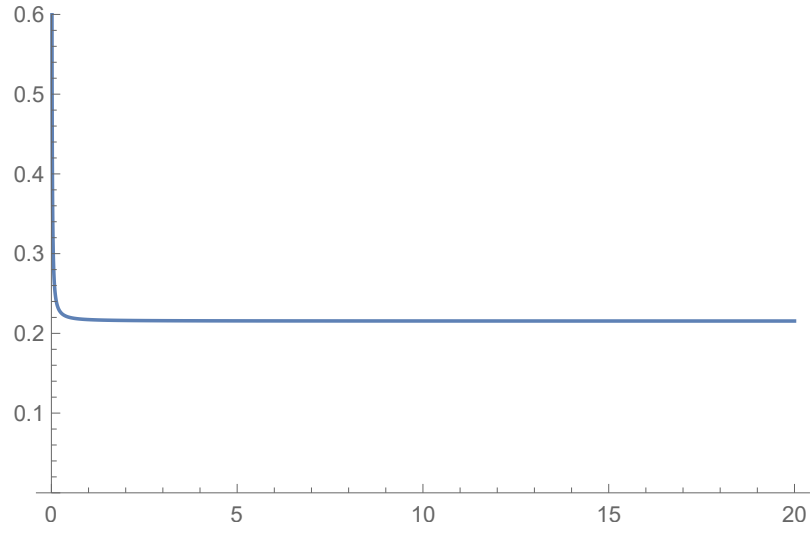


Figure 4.3: Sound speed ( $\frac{dp}{d\rho}$ ) versus radius ( $r$ ).

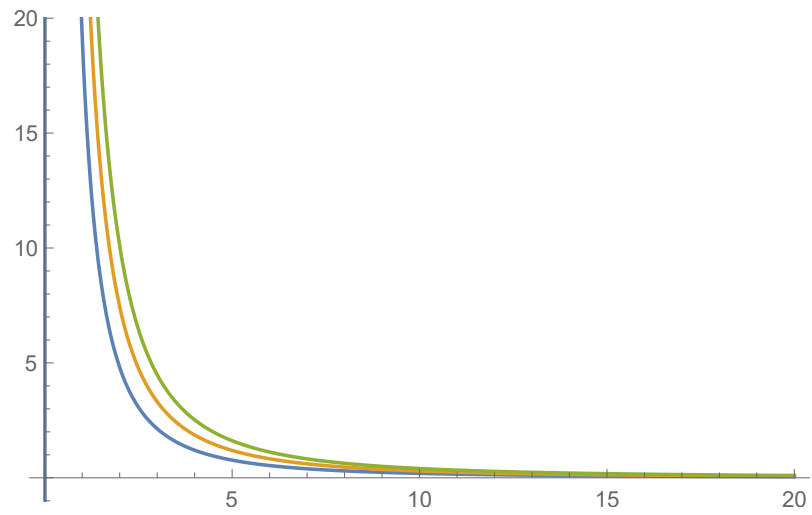


Figure 4.4: Energy conditions ( $\rho - p$ ,  $\rho + p$ ,  $\rho + 3p$ ) versus radius ( $r$ ).

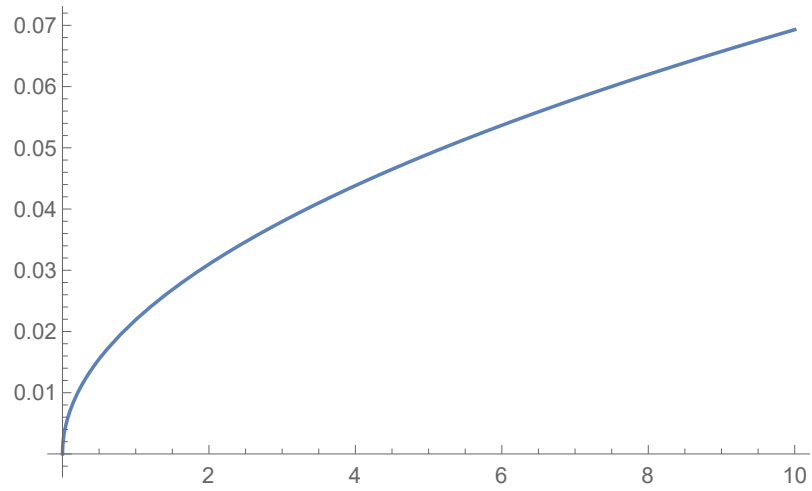


Figure 4.5: Gravitational mass ( $m(r)$ ) versus radius ( $r$ ).

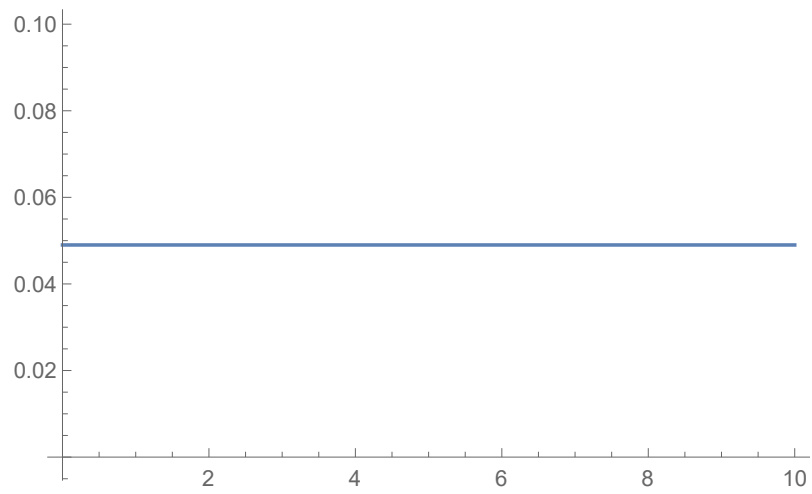


Figure 4.6: Compactification parameter ( $\frac{m}{r}$ ) versus radius ( $r$ ).

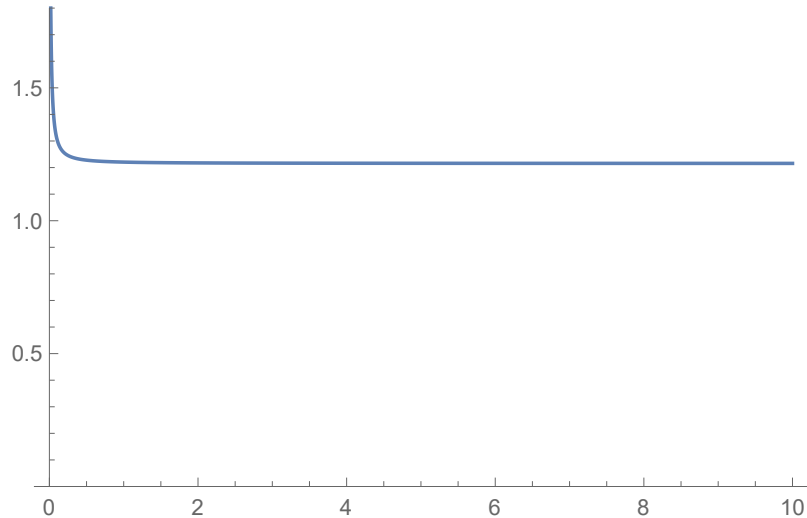


Figure 4.7: Chandrasekhar adiabatic stability index  $\left(\frac{\rho+p}{p}\right) \frac{dp}{d\rho}$  versus radius ( $r$ ).

In order to examine our model graphically, the following parameter choices were made:  $K = 0$ ,  $C = 5$ ,  $A = 0.025$ ,  $k = 0.3$  and  $B = 100$ . Plots of the dynamical quantities have been generated with the aid of the computer system Wolfram Mathematica 11.3. Figure 4.1 and 4.2 demonstrates the behaviour of the energy density and pressure when put against the radius, we can observe that they are both positive and monotonically decreasing functions respectively. In figure 4.3 we observe that the causality principle  $0 \leq \frac{dp}{d\rho} \leq 1$  has been violated at the centre ( $r = 0$ ) of the star. Figure 4.4 shows that all energy conditions are satisfied everywhere within the sphere since they are all positive. A plot of gravitational mass is shown in figure 4.5. A positive but constant compactification parameter plot is shown in figure 4.6, but most importantly the causality principle  $\frac{m}{r} < \frac{4}{9}$  holds. Figure 4.7 represents the behaviour of the Chandrasekhar adiabatic stability index when put against radius. We observe that it is unstable as we expected it to be always  $> \frac{4}{3}$ . Additionally, it is singular at the centre.

#### 4.2.4 Finch–Skea model: $Z = \frac{1}{1+x}$

The special case  $a = 0$ ,  $b = 1$  of the Vaidya–Tikekar ansatz (4.7) corresponds to the Finch–Skea prescription. Introducing  $Z = \frac{1}{x+1}$  equation (4.1) reduces to the simpler form

$$4(1+x)\ddot{y} - 6\dot{y} + y = 0 \quad (4.25)$$

which can be transformed to Bessel or modified Bessel form. With the substitution  $V = 1+x$  equation (4.25) assumes the form

$$4Vy'' - 6y' + y = 0 \quad (4.26)$$

The substitution  $y(V) = u(V)V^m$  where  $u(V)$  is a function and  $m$  is a real number, further transforms (4.26) to

$$4V^2\ddot{u} + (8m-6)V\dot{u} + (4m^2 - 10m + V)u = 0 \quad (4.27)$$

where dots are derivatives with respect to  $V$ . Introducing the additional transformation  $w = V^\beta$  and  $\beta$  is a real number, we obtain the form

$$4\beta^2 V^{2\beta} \frac{d^2 u}{dw^2} + [4\beta(\beta-1) + (8m-6)\beta] V^\beta \frac{du}{dw} + (4m^2 - 10m + V)u = 0 \quad (4.28)$$

for equation (4.27).

The choices  $m = 1$  and  $\beta = \frac{1}{2}$ , simplify equation (4.28) to the form

$$w^2 \frac{d^2 u}{dw^2} + (w^2 - 6)u = 0 \quad (4.29)$$

where the first order derivative is now absent. Equation (4.29) is the Bessel equation of order 2 and can be solved by the spherical Bessel functions  $J_2(w)$  and  $Y_2(w)$  as

$$u = c_1 J_2 + c_2 Y_2 \quad (4.30)$$

where  $c_1$  and  $c_2$  are constants. It is well known that for half-integer order, Bessel functions are reducible to elementary functions. In this case solutions may be written as

$$u(w) = a \left[ \frac{3 \sin w - w^2 \sin w - 3w \cos w}{w^2} \right] + b \left[ \frac{w^2 \cos w - 3 \cos w - 3w \sin w}{w^2} \right] \quad (4.31)$$

where  $a = \sqrt{\frac{2}{\pi}}c_1$  and  $b = \sqrt{\frac{2}{\pi}}c_2$  are arbitrary constants. Recall that  $w = V^{\frac{1}{2}} = \sqrt{1+x}$ . The gravitational potentials and dynamic quantities have the form

$$e^\lambda = w = \sqrt{1+Cr^2} \quad (4.32)$$

$$e^\nu = [a(3-w^2) - 3bw] \sin w + [b(w^2-3) - 3aw] \cos w \quad (4.33)$$

$$\rho = \frac{12(w^2+4)}{w^6} \quad (4.34)$$

$$p = \frac{2[(\zeta w - w^2 - 1) \tan w + \zeta(w^2 + 1) + w]}{w^6 [(w^2 - 3 + 3\zeta w) \tan w - \zeta(w^2 - 3) + 3w]} \quad (4.35)$$

where we have set  $\zeta = \frac{a}{b}$  and  $C = 1$ . A comprehensive study of this solution is found in [19] [23] and is therefore not pursued here in detail. In this paper the authors demonstrated a remarkable similarity between the graphical profiles of 4D Einstein and 6D pure Gauss–Bonnet theory.

#### 4.2.5 New special cases

On examining the Vaidya–Tikekar general solution (4.9) it is noteworthy that the choice  $b = 5a$  simplifies the hypergeometric functions and a family of solutions in

terms of elementary functions may be realised. Substituting

$$Z = \frac{1 + ax}{1 + 5ax} \quad (4.36)$$

into (4.1) yields the simplified equation

$$(5a^2x^2 + 6ax + 1) \ddot{y} - a(5ax + 7)\dot{y} + 5a^2y = 0 \quad (4.37)$$

which is solved by

$$y = A(5ax + 7) + \frac{B}{5a} \left( -15\sqrt{ax+1}\sqrt{5ax+1} + h\sqrt{5}(5ax+7) \right) \quad (4.38)$$

where  $h = \log(-5ax - \sqrt{5ax+1}\sqrt{5ax+5} - 3)$ ,  $A$  and  $B$  are constants of integration.

For this exact solution the energy density and pressure are given by

$$\frac{\rho}{C^2} = \frac{160a^2(ax+1)}{(5ax+1)^3} \quad (4.39)$$

$$\begin{aligned} \frac{p}{C^2} = & \left( 32 \left( 5 \left( 5a^2Axh_1 + 3aAh_1 - aBxh_2 - Bh_2 \right) + hB(5ax+3)\sqrt{5ax+5} \right) \right. \\ & \left. \left( 5 \left( 5a^2Ax + 7aA - 3Bh_1h_2 \right) + h\sqrt{5}B(5ax+7) \right) \right) / \left( 25h_1(5ax+1)^2 \right) \end{aligned} \quad (4.40)$$

where we have redefined  $h = \log(-5ax - h_2\sqrt{5ax+5} - 3)$ ,  $h_1 = \sqrt{ax+1}$  and  $h_2 = \sqrt{5ax+1}$ . Observe that there are no singularities at the stellar centre  $x = 0 = r$ .

The square of the sound speed has the form

$$\begin{aligned} \frac{dp}{d\rho} = & h_2 \left( 20B^2(5ax+4) \left( 5\sqrt{5}a^2x^2 + ax \left( 5h_1h_2 + 6\sqrt{5} \right) + 3h_1h_2 + \sqrt{5} \right) h^2 \right. \\ & \left. - Bh \left( 625a^4x^3 \left( \sqrt{5}Bx - 8A \right) - 125a^3x^2 \left( 8A \left( h_2\sqrt{5ax+5} + 10 \right) \right) \right) \right) \end{aligned}$$

$$\begin{aligned}
& -Bx \left( 5h_1h_2 + 24\sqrt{5} \right) - 25a^2x \left( 8A \left( 7h_2\sqrt{5ax+5} + 29 \right) \right. \\
& -15Bx \left( 7h_1h_2 + 10\sqrt{5} \right) - 160aA \left( 3h_2\sqrt{5ax+5} + 5 \right) \\
& +5aBx \left( 435h_1h_2 + 328\sqrt{5} \right) + 67B \left( 5h_1h_2 + 3\sqrt{5} \right) \\
& +5 \left( 125a^5Ax^3 \left( 4\sqrt{5}A - 5Bx \right) + 125a^4x^2 \left( 4A^2 \left( h_1h_2 + 2\sqrt{5} \right) \right. \right. \\
& -ABx \left( h_2\sqrt{5ax+5} + 24 \right) + 2\sqrt{5}B^2x^2 \left. \right) + 5a^3x \left( 4A^2 \left( 35h_1h_2 + 29\sqrt{5} \right) \right. \\
& -15ABx \left( 7h_2\sqrt{5ax+5} + 50 \right) + 10B^2x^2 \left( 5h_1h_2 + 14\sqrt{5} \right) \\
& +5a^2 \left( 16A^2 \left( 3h_1h_2 + \sqrt{5} \right) - ABx \left( 87h_2\sqrt{5ax+5} + 328 \right) \right. \\
& +10B^2x^2 \left( 11h_1h_2 + 12\sqrt{5} \right) \left. \right) + aB \left( 2Bx \left( 155h_1h_2 + 82\sqrt{5} \right) \right. \\
& -67A \left( h_2\sqrt{5ax+5} + 3 \right) \\
& \left. \left. +14B^2 \left( 3h_1h_2 + \sqrt{5} \right) \right) \right) / \left( 25a^2h_1(5ax+7) \left( 5ax + h_2\sqrt{5ax+5} + 3 \right) \right)
\end{aligned} \tag{4.41}$$

The 6D mass has the form

$$m = \frac{8a^2\sqrt{x^5}(1+ax)}{\sqrt{C}(1+5ax)^3} + K \tag{4.42}$$

where  $K$  is a constant of integration.

Extensive empirical testing of the above solution suggests that we may not be able to find suitable parameter values such that all elementary requirements are met. We have attempted to find such parameter values by a process of careful fine-tuning of the constants. Consulting our table 4.1 we find that the potential

$$Z = \frac{1-x}{1+11x} \tag{4.43}$$

gives the temporal metric potential in the form

$$y = A\sqrt{1-x}(11x+1)^{5/2} + B(1331x^3 - 363x^2 - 297x - 131) \quad (4.44)$$

which is singularity free. The associated physical quantities are now given by the following expressions. The energy density and pressure have the forms

$$\rho = \frac{288(11x+5)}{(11x+1)^3} \quad (4.45)$$

$$\begin{aligned} p = & -864. \left( (h - 0.294545u)x^3 + (0.419504u - 0.878788h)x^2 \right. \\ & \left. - (0.00275482h + 0.111165u)x + (0.0167794h - 0.0137941u) \right) \\ & / h(11x+1)^2 \left( x^3 + (0.294545hu - 0.272727)x^2 \right. \\ & \left. + (0.0535537hu - 0.22314)x + (0.00243426hu - 0.0984222) \right) \quad (4.46) \end{aligned}$$

respectively and where we have put  $h = \sqrt{1-x}$ ,  $u = \sqrt{11x+1}$  and  $v = hu$  to simplify the expressions. The sound speed squared is given by

$$\begin{aligned} \frac{dp}{d\rho} = & 224.074(1x + 0.0909091) \left( (0.0237542 - 0.00297662v)x^2 \right. \\ & \left. + (0.00297693 - 0.00217598v)x - (0.00704826v + 2.90909)x^7 \right. \\ & \left. + (0.0173003v + 2.6281)x^6 - (0.0117083v + 0.453794)x^5 \right. \\ & \left. - (0.0000264773v + 0.318284)x^4 + (0.00692658v + 0.0262277)x^3 \right. \\ & \left. - 0.000291251v + 1x^8 + 0.000111304 \right) \\ & / hu(x-1)(1x + 0.636364) \left( (1v - 0.925926)x^2 \right. \\ & \left. + (0.181818v - 0.757576)x + 0.00826446v + 3.39506x^3 - 0.33415 \right)^2 \quad (4.47) \end{aligned}$$

The energy conditions may be studied with the help of the expressions

$$\begin{aligned}
\rho - p &= 864. \left( (h - 0.294545u)x^3 + (0.419504u - 0.878788h)x^2 \right. \\
&\quad \left. - (0.00275482h + 0.111165u)x + (0.0167794h - 0.0137941u) \right) \\
&\quad / h(11.x + 1.)^2 \left( x^3 + (0.294545v - 0.272727)x^2 \right. \\
&\quad \left. + (0.0535537v - 0.22314)x + (0.00243426v - 0.0984222) \right) \\
&\quad + \frac{288(11x + 5)}{(11x + 1)^3} \tag{4.48}
\end{aligned}$$

$$\begin{aligned}
\rho + p &= -864. \left( (h - 0.294545u)x^3 + (0.419504u - 0.878788h)x^2 \right. \\
&\quad \left. - (0.00275482h + 0.111165u)x + (0.0167794h - 0.0137941u) \right) \\
&\quad / h(11.x + 1.)^2 \left( x^3 + (0.294545v - 0.272727)x^2 \right. \\
&\quad \left. + (0.0535537v - 0.22314)x + (0.00243426v - 0.0984222) \right) \\
&\quad + \frac{288(11x + 5)}{(11x + 1)^3} \tag{4.49}
\end{aligned}$$

$$\begin{aligned}
\rho + 3p &= -2592. \left( (h - 0.294545u)x^3 + (0.419504u - 0.878788h)x^2 \right. \\
&\quad \left. - (0.00275482h + 0.111165u)x. + (0.0167794h - 0.0137941u) \right) \\
&\quad / h(11.x + 1.)^2 \left( x^3 + (0.294545v - 0.272727)x^2 \right. \\
&\quad \left. + (0.0535537v - 0.22314)x + (0.00243426v - 0.0984222) \right) \\
&\quad + \frac{288(11x + 5)}{(11x + 1)^3} \tag{4.50}
\end{aligned}$$

The gravitational mass is given by

$$m = \frac{360x^{5/2} + 792x^{7/2} + 6655x^3 + 1815x^2 + 165x + 5}{5(11x + 1)^3} \tag{4.51}$$

Utilising the parameter values  $A = 0,001$ ,  $B = 1$ ,  $C = 1$  and  $K = 1$  we are able

to generate the following graphical plots of the physical quantities.

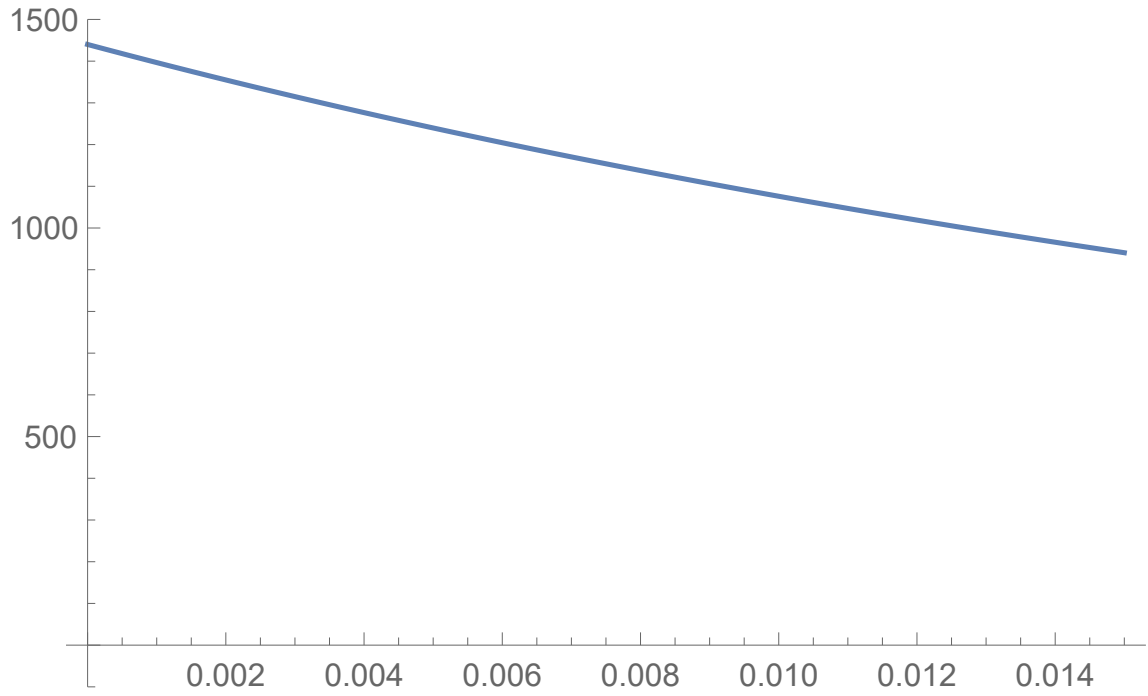


Figure 4.8: Density ( $\rho$ ) versus radius ( $r$ ).

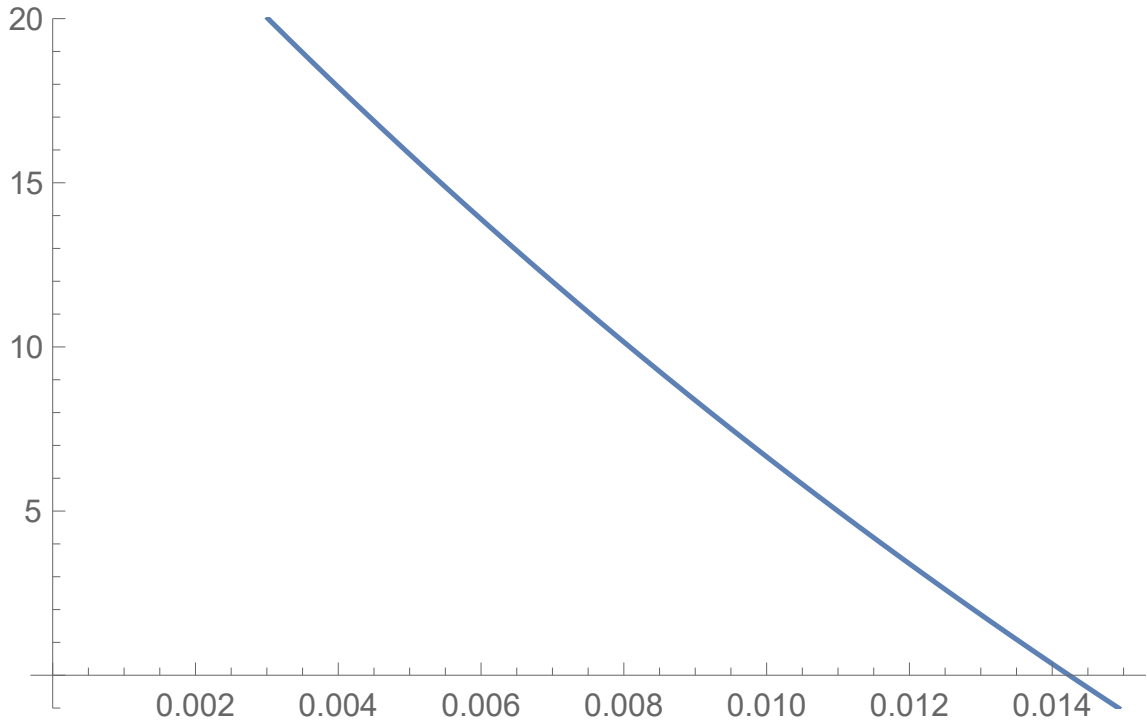


Figure 4.9: Pressure ( $p$ ) versus radius ( $r$ ).

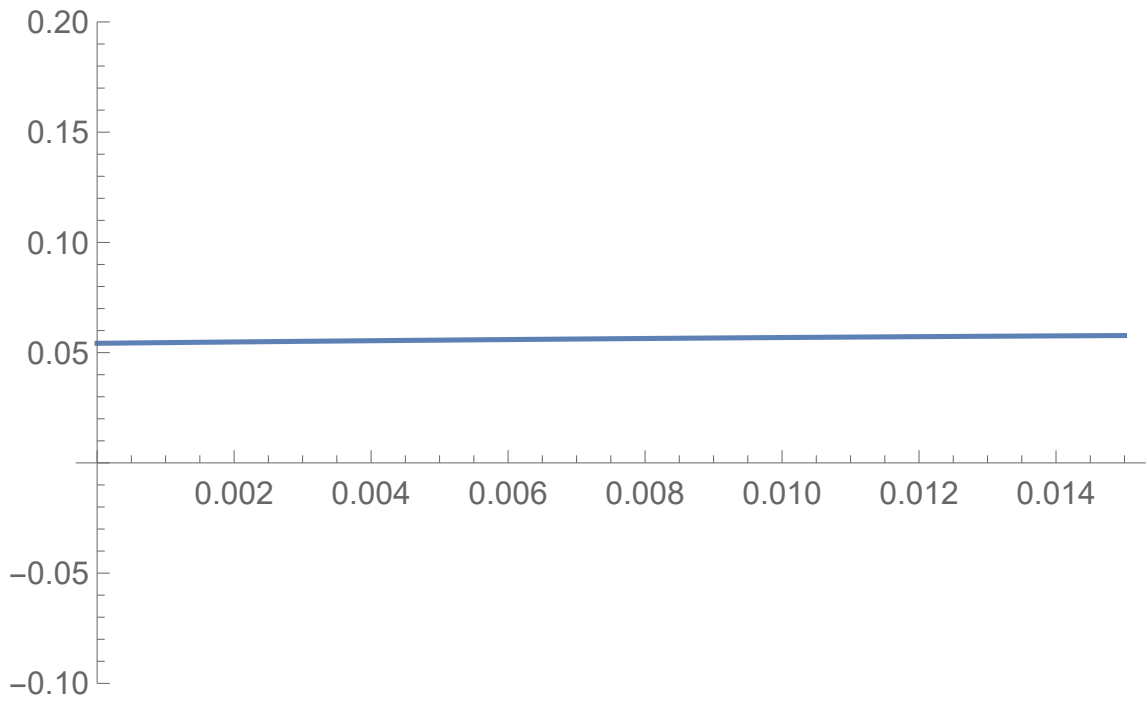


Figure 4.10: Sound speed ( $\frac{dp}{d\rho}$ ) versus radius ( $r$ ).

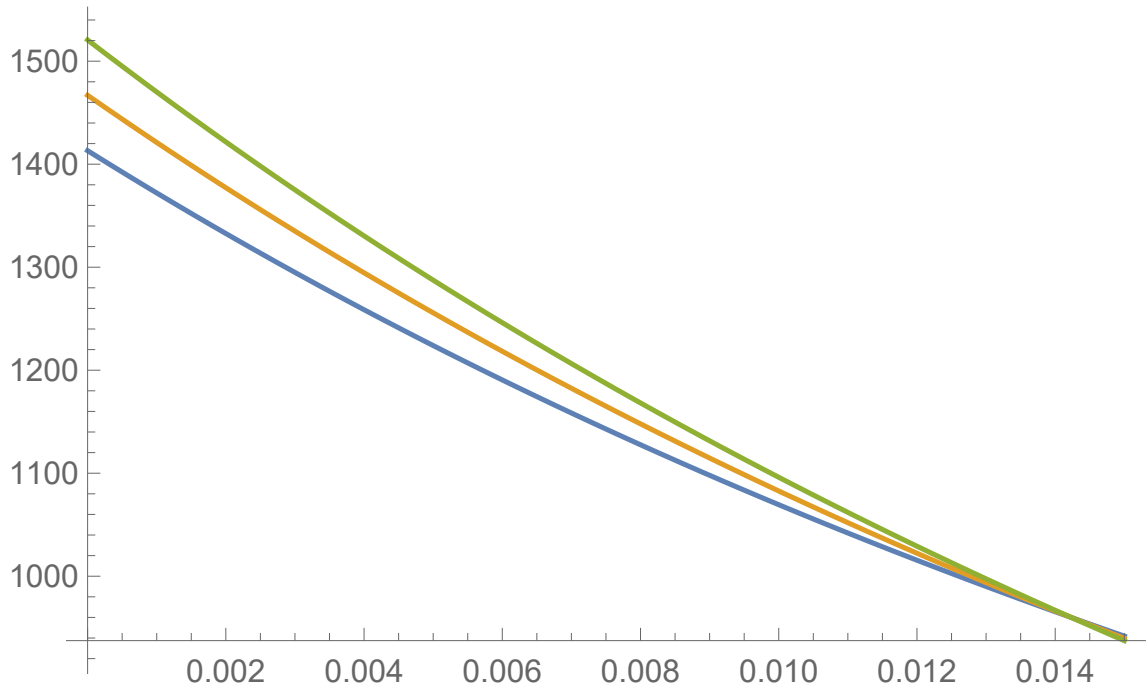


Figure 4.11: Energy conditions ( $\rho - p$ ,  $\rho + p$ ,  $\rho + 3p$ ) versus radius ( $r$ ).

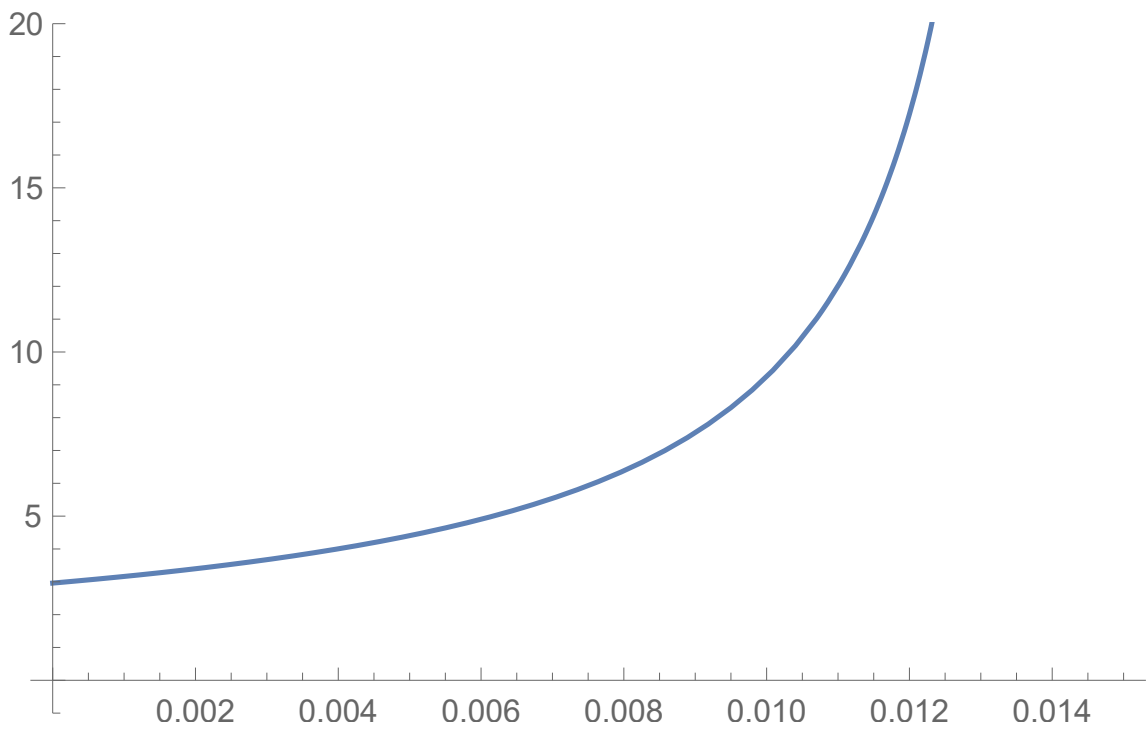


Figure 4.12: Chandrasekhar adiabatic stability index  $\left(\frac{\rho+p}{p}\right) \frac{dp}{d\rho}$  versus radius ( $r$ ).

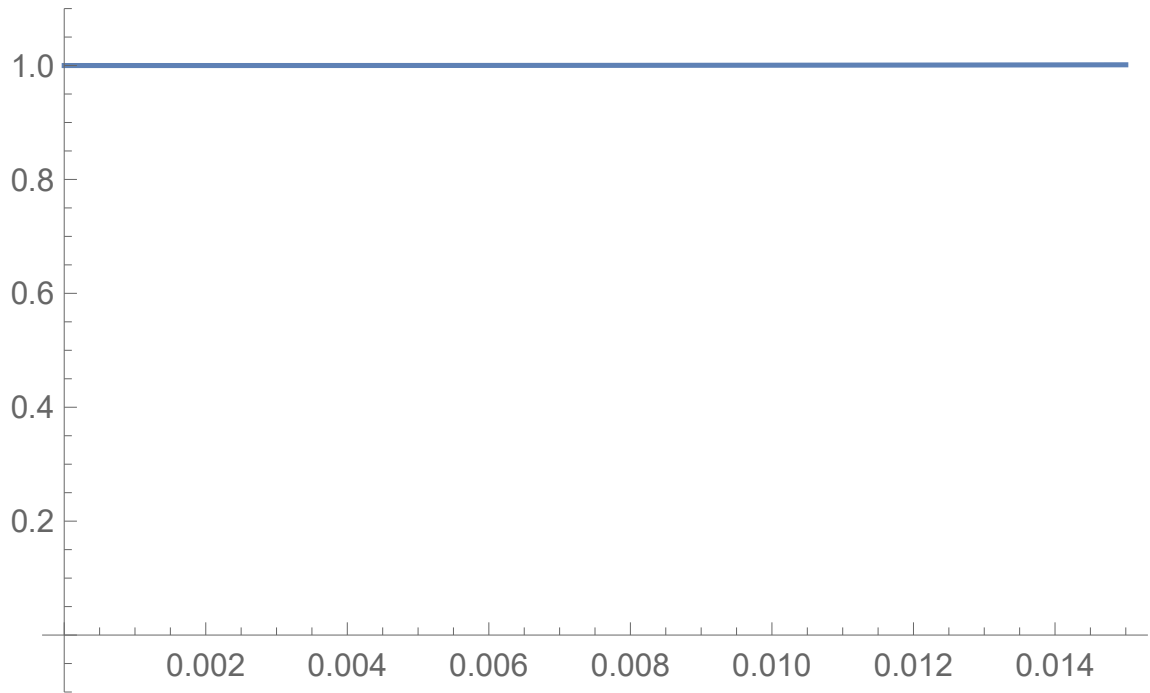


Figure 4.13: Gravitational mass ( $m(r)$ ) versus radius ( $r$ ).

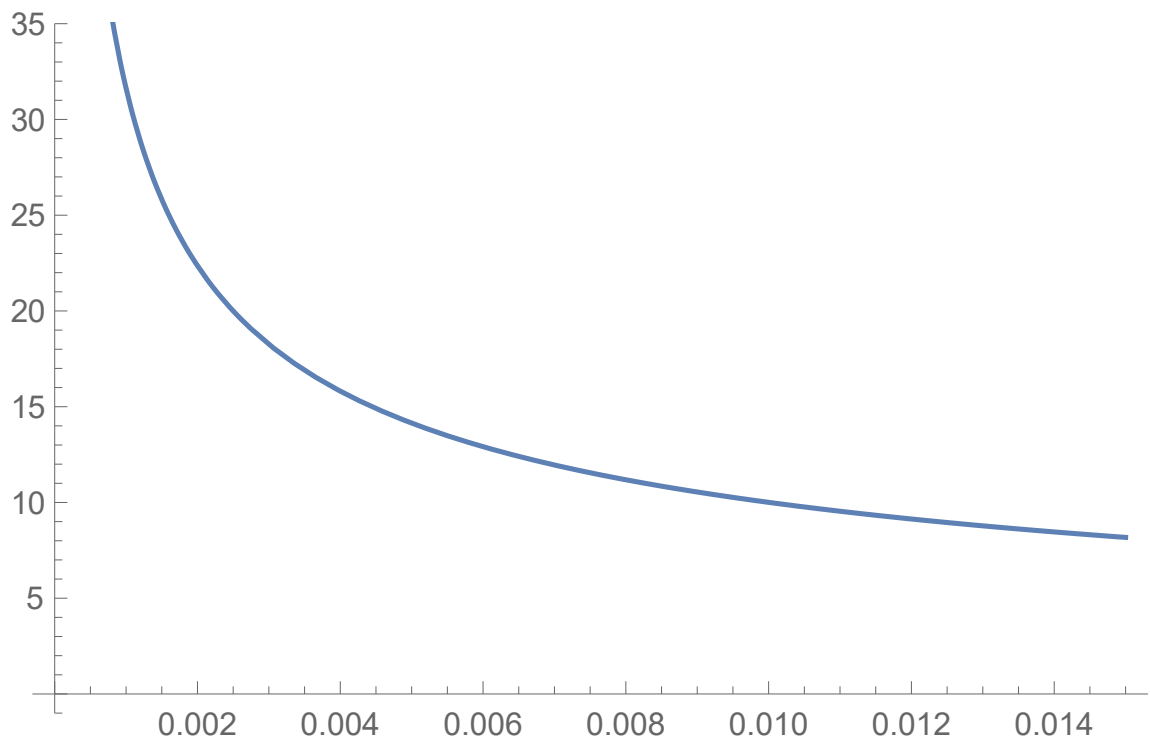


Figure 4.14: Compactification parameter ( $\frac{m}{r}$ ) versus radius ( $r$ ).

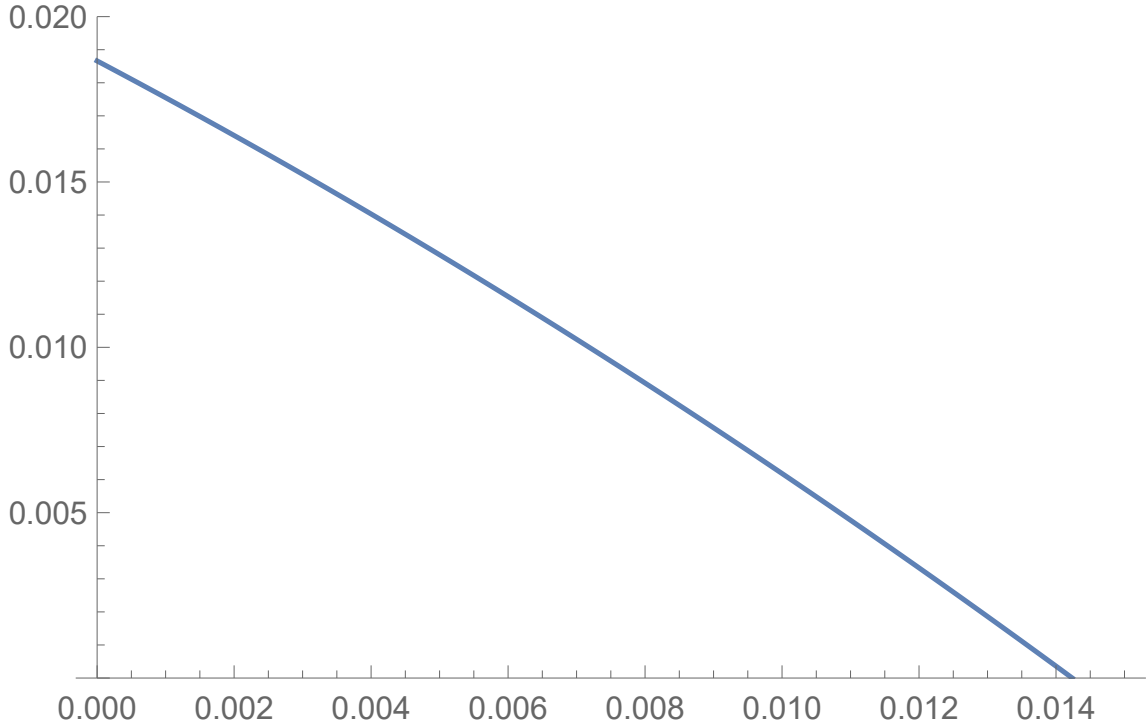


Figure 4.15: Equation of state ( $\frac{p}{\rho}$ ) versus radius ( $r$ ).

We used the computer system Wolfram Mathematica 11.3 to generate the plots for the physical quantities. The plots show important information about the physical properties of our model and its practicality. Figure 4.8 shows how the energy density ( $\rho$ ) behaves reasonably when varied against the radial coordinate ( $r$ ). The energy density is a monotonically decreasing function from the center of the fluid as the radius increases. Figure 4.9 shows how the pressure ( $p$ ) behaves versus radius ( $r$ ). It clearly can be observed that the pressure is positive at the origin, becomes zero at  $r = 0.0141$  and decreases monotonically outwards from the centre. This vanishing pressure shows that the distribution has a finite radius. Figure 4.10 is a plot of the sound speed ( $\frac{dp}{d\rho}$ ) versus radius ( $r$ ). It can be observed that the sound speed profile satisfies the condition  $0 \leq \frac{dp}{d\rho} \leq 1$  and this demonstrates that the sound speed remains lower than the light speed. Figure 4.11 shows the energy conditions against radius. These plots clearly show that the weak, strong and dominant en-

ergy conditions are satisfied everywhere within the spherical distribution as can be observed that they are all positive. Figure 4.12 shows the relationship between the Chandrasekhar adiabatic stability index and the radius. We can observe that the adiabatic stability criterion in the Gauss–Bonnet context is achieved:  $\left(\frac{\rho+p}{p}\right) \frac{dp}{d\rho} \geq \frac{4}{3}$ . Figure 4.13 represents a constant but positive gravitational mass as expected. Figure 4.14 shows the plot of the compactification parameter  $\left(\frac{m}{r}\right)$ , monotonically decreasing as the radius increases. Figure 4.15 shows the equation of state. The pressure has been expressed as a function of the density. From the analysis of our plots, it can be concluded that this model indeed does satisfy the elementary requirements for realistic behaviour. It therefore has potential to model realistic objects and in future work attempts will be made to match it with known stars.

## 4.2.6 Conformal Killing vector

As explained in Chapter 3, it has been established by several researchers that a condition for the existence of a conformal Killing vector is that the temporal potential varies proportionally with the square of the radius. This means that  $e^{2\nu} \sim r^2$  or in this case  $y \sim x$ .

Using our transformed co-ordinates where  $y = ax$  is substituted in equation (4.1) we get

$$3x\dot{Z} - 7xZ\dot{Z} - 6Z + 5Z^2 + 1 = 0 \quad (4.52)$$

which is a nonlinear first order differential equation in  $Z(x)$ . Equation (4.52) may be rearranged in the form

$$(7Z - 3)\dot{Z} = \frac{5}{x}Z^2 - \frac{6}{x}Z + \frac{1}{x} \quad (4.53)$$

to cast it in the standard Abelian form.

Implementing the sequence of transformations in [35] for ordinary differential equations of the form,

$$[g_1(x)Z + g_0(x)]\dot{Z} = f_2(x)Z^2 + f_1(Z) + f_0(x) \quad (4.54)$$

with the substitution of

$$w = \left( Z + \frac{g_0}{g_1} \right) E \quad (4.55)$$

where

$$E = \exp\left(-\int \frac{f_2}{g_1} dx\right), \quad (4.56)$$

equation (4.54) can be reduced to the form

$$w\dot{w}_x = F_1(x)w + F_0(x) \quad (4.57)$$

where

$$F_1 = \left[ \frac{d}{dx} \left( \frac{g_0}{g_1} \right) + \frac{f_1}{g_1} - 2 \frac{g_0 f_2}{g_1^2} \right] E \quad (4.58)$$

$$F_2 = \left( \frac{f_0}{g_1} - \frac{g_0 f_1}{g_1^2} + \frac{g_0^2 f_2}{g_1^3} \right) E^2. \quad (4.59)$$

In our case the relevant substitutions render equation (4.54) as

$$Z\dot{Z} = -\frac{12}{49}x^{-\frac{12}{7}}Z - \frac{32}{343}x^{-\frac{17}{7}} \quad (4.60)$$

Next introducing the transformation

$$\xi = -6 \ln(x) \quad (4.61)$$

equation (4.60) assumes the form

$$Z \frac{dZ}{d\xi} = Z - \frac{1}{6} \quad (4.62)$$

which has the solution

$$x = Z + \frac{1}{6} \ln \left| Z - \frac{1}{6} \right| + K \quad (4.63)$$

where  $K$  is a constant of integration. We have thus found an exact solution although it is in implicit form. Further study of this solution is impeded as we do not have an explicit solution. It is also not known what the form of the conformal factor will be.

### 4.2.7 Inverse square law for the temporal potential

In searching for new exact solutions we consider other potentials. Inserting  $y = \frac{1}{x}$  in equation (4.1) generates the condition

$$5x\dot{Z}Z - x\dot{Z} - 11Z^2 - 10Z + 1 = 0 \quad (4.64)$$

which is nonlinear. Rearranging (4.64) we obtain

$$(5Z - 1)\dot{Z} = \frac{11}{x}Z^2 + \frac{10}{x}Z - \frac{1}{x}. \quad (4.65)$$

Again using the procedures outlined in the previous section we are able to write equation (4.65) as

$$Z\dot{Z} = -\frac{228}{25}Z + \frac{164}{125}x^{21}. \quad (4.66)$$

Putting

$$\xi = 10 \ln(x) \quad (4.67)$$

we find the reduced equation of the form

$$Z \frac{dZ}{d\xi} = Z - \frac{1}{10} \quad (4.68)$$

which gives us the implicit solution

$$x = Z + \frac{1}{10} \ln \left| Z - \frac{1}{10} \right| + K \quad (4.69)$$

where  $K$  is a constant of integration. Once again we find that we are unable to proceed with a detailed physical analysis. Approximate explicit solutions are possible but our purpose is to study exact solutions to build viable models representing realistic matter.

### 4.3 Conclusion

In this chapter, we analyzed the pressure isotropy condition and established new exact solutions for the pure Gauss–Bonnet equations of motion in  $6D$ . We have found that closed hyperspheres of perfect fluids exist for  $D = 6$  in pure Lovelock gravity as expected. A variety of choices of the metric potentials that generated exact solutions were considered. Special cases of the Vaidya–Tikekar ansatz, the Finch–Skea metric, the Schwarzschild interior metric as well as the isothermal fluid were studied. Lastly, it was shown that the condition for the existence of a conformal Killing vector that the temporal potential varies proportionally with the square of the radius led to an implicit solution. Other potentials were also considered. The inverse square law for the temporal potential was examined but we could not continue with the detailed physical analysis since only implicit solutions were found. Approximate explicit solutions were possible but the motive was to study exact solutions to build viable models representing realistic matter. We have demonstrated at least one exact model which satisfied all elementary physical requirements extrapolated from the theory of Einstein.

# Chapter 5

## Third Order Lovelock Polynomial

### 5.1 Introduction

In the previous 2 chapters we have examined the  $N = 2$  pure Lovelock polynomial in 5 and 6 dimensions referred to as the Gauss–Bonnet case. This order of Lovelock polynomial is well motivated as the Gauss–Bonnet term appears in the action of string theory. In this chapter we consider the most general Lovelock polynomials for all  $N$  and  $d$  values but for the critical spacetime dimensions  $d = 2N + 1$  and  $d = 2N + 2$ . Thereafter we specialise to the cases  $N = 3$ ,  $d = 7$  and  $d = 8$  which have not been considered previously in the literature. Admittedly, the physical motivations for this case are not very clear at this stage. However, analysing this case will deepen our understanding of the influence of higher curvature terms in the evolution of stellar structure. In this context, the governing equations are more complicated than the Gauss–Bonnet case. A comprehensive treatment lies outside the ambit of this dissertation, so a full physical analysis of solutions is not conducted.

## 5.2 The general Lovelock case $d = 2N + 1$

The pressure isotropy in equation (2.27) has the form

$$4x^2 Z (1 - Z) \ddot{y} + \left[ 4(1 - N) x Z (1 - Z) + 2x^2 (1 - (2N - 1) Z) \dot{Z} \right] \dot{y} \\ + (d + 2N - 1) (1 - Z) (\dot{Z} x - Z + 1) y = 0 \quad (5.1)$$

for all spacetime dimensions  $d$  and Lovelock polynomials of order  $N$ .

Putting  $d = 2N + 1$  in the above equation (5.1) gives

$$2xZ (1 - Z) \ddot{y} + \left[ 2(1 - N) Z (1 - Z) + x (1 - (2N - 1) Z) \dot{Z} \right] \dot{y} = 0 \quad (5.2)$$

and a first integral of (5.2) is

$$\dot{y} = \frac{Ax^{N-1} (1 - Z)^{1-N}}{\sqrt{Z}} \quad (5.3)$$

or in general

$$y = A \int \frac{x^{N-1} (1 - Z)^{1-N}}{\sqrt{Z}} dx + B \quad (5.4)$$

where  $A$  and  $B$  are constants of integration. Thus for  $d = 2N + 1$  the gravitational potentials are related through equation (5.4).

We now consider some of the special cases of physical interest. The Vaidya–Tikekar prescription

$$Z = \frac{1 + ax}{1 + bx} \quad (5.5)$$

which generates the exact solution

$$y = 2A\sqrt{ax + 1}(bx + 1)^{N-\frac{1}{2}} \left( \frac{abx + a}{a - b} \right)^{\frac{1}{2}-N}$$

$${}_2F_1\left(\frac{1}{2}, \frac{1}{2} - N; \frac{3}{2}; -\frac{axb+b}{a-b}\right)/a + B \quad (5.6)$$

through equation (5.4) and where  ${}_2F_1$  is the hypergeometric function.

For  $a = 1$ ,  $b = 0$  we get

$$y = 2A\sqrt{x+1} + B \quad (5.7)$$

which is the Schwarzschild Interior solution as expected.

For  $a = 0$  and  $b = 1$  we get

$$y = \frac{2A(x+1)^{N+\frac{1}{2}}}{2N+1} + B \quad (5.8)$$

which corresponds to the Finch-Skea solution in  $d = 2N + 1$  spacetime dimensions.

The case  $a = 2$  and  $b = -1$  which is the only case that was considered by Vaidya and Tikekar, results in the exact solution

$$y = A\left(\frac{2}{3}\right)^{\frac{1}{2}-N} \sqrt{2x+1} {}_2F_1\left(\frac{1}{2}, \frac{1}{2} - N; \frac{3}{2}; \frac{1}{3}(2x+1)\right) + B \quad (5.9)$$

still containing the hypergeometric functions. Specialising to  $N = 3$  and  $d = 7$ , we get

$$\begin{aligned} y = & \frac{1}{384}A\left(2\sqrt{(1-x)(2x+1)}(32x^2 - 124x + 227)\right. \\ & \left. - 405\sqrt{2}\sin^{-1}\left(\sqrt{\frac{2}{3}}\sqrt{1-x}\right)\right) + B \end{aligned} \quad (5.10)$$

in terms of elementary functions. The energy density and pressure are given by

$$\frac{\rho}{C^3} = -\frac{405}{(x-1)^4} \quad (5.11)$$

$$\begin{aligned}
\frac{p}{C^3} &= (270A\sqrt{2x+1}) \\
&/x \left( \sqrt{1-x} \left( \frac{1}{384}A \left( 2\sqrt{1-x}\sqrt{2x+1} (32x^2 - 124x + 227) \right. \right. \right. \\
&\quad \left. \left. \left. -405\sqrt{2} \sin^{-1} \left( \sqrt{\frac{2}{3}}\sqrt{1-x} \right) \right) + B \right) \right)
\end{aligned} \tag{5.12}$$

respectively. The sound speed squared has the form

$$\frac{dp}{d\rho} = \frac{A(1-x)^{13/2}(8x+7)}{3240(2x+1)^{3/2}} \tag{5.13}$$

While the expressions relevant to the energy conditions have the form

$$\begin{aligned}
\frac{\rho - p}{C^3} &= - \left( 270A\sqrt{2x+1}/x \left( \sqrt{1-x} \left( \frac{1}{384}A \left( 2\sqrt{(1-x)(2x+1)} (32x^2 - 124x + 227) \right. \right. \right. \right. \\
&\quad \left. \left. \left. -405\sqrt{2} \sin^{-1} \left( \sqrt{\frac{2}{3}}\sqrt{1-x} \right) \right) + B \right) \right) \right) - \frac{405C^3}{(x-1)^4}
\end{aligned} \tag{5.14}$$

$$\begin{aligned}
\frac{\rho + p}{C^3} &= 270A\sqrt{2x+1}/x \left( \sqrt{1-x} \left( \frac{1}{384}A \left( 2\sqrt{1-x}\sqrt{2x+1} (32x^2 - 124x + 227) \right. \right. \right. \\
&\quad \left. \left. \left. -405\sqrt{2} \sin^{-1} \left( \sqrt{\frac{2}{3}}\sqrt{1-x} \right) \right) + B \right) \right) - \frac{405C^3}{(x-1)^4}
\end{aligned} \tag{5.15}$$

$$\begin{aligned}
\frac{\rho + 3p}{C^3} &= 810A\sqrt{2x+1}/x \left( \sqrt{1-x} \left( \frac{1}{384}A \left( 2\sqrt{1-x}\sqrt{2x+1} (32x^2 - 124x + 227) \right. \right. \right. \\
&\quad \left. \left. \left. -405\sqrt{2} \sin^{-1} \left( \sqrt{\frac{2}{3}}\sqrt{1-x} \right) \right) + B \right) \right) - \frac{405C^3}{(x-1)^4}
\end{aligned} \tag{5.16}$$

corresponding to the weak, strong and dominant energy conditions respectively. It is well known that  $d = 2N + 1$  solutions cannot yield bounded distributions so we do not consider this case deeply.

### 5.3 The case $d = 2N + 2$

Putting  $d = 2N + 2$  in (5.1) gives the equation

$$\begin{aligned}
 4x^2 Z (1 - Z) \ddot{y} + \left[ 4(1 - N) x Z (1 - Z) + 2x^2 (1 - (2N - 1) Z) \dot{Z} \right] \dot{y} \\
 + (1 - Z) (\dot{Z} x - Z + 1) y = 0
 \end{aligned}
 \tag{5.17}$$

which is a linear second order differential equation in  $y$  but a nonlinear equation in  $Z$ . Hence Lovelock isotropy equations are said to generate quasi-linear equations of motion. In this case it is not possible to separate and find the exact solution of  $y$  in terms of  $Z$ .

We again look at the Vaidya–Tikekar prescription which gives us the exact solution

$$\begin{aligned}
 y = & \sqrt[4]{\frac{1}{a} + x} \left( \frac{1}{b} + x \right)^{\frac{1}{4}(1-2N)} (bx + 1)^{\frac{N}{2} - \frac{1}{4}} \\
 & \left( A {}_2F_1 \left( \frac{Q - aN}{2a}, -\frac{aN + Q}{2a}; \frac{1}{2}; -\frac{axb + b}{a - b} \right) \right. \\
 & \left. + B \sqrt{\frac{abx + b}{a - b}} {}_2F_1 \left( -\frac{a(N - 1) + Q}{2a}, \frac{-Na + a + Q}{2a}; \frac{3}{2}; -\frac{axb + b}{a - b} \right) \right) \\
 & / \sqrt[4]{ax + 1}
 \end{aligned}
 \tag{5.18}$$

where  $Q = \sqrt{a(aN^2 + a - b)}$  and  $A, B$  are constants of integration.

Specialising to  $N = 3, d = 8$  we get

$$y = b \sqrt[4]{\frac{1}{a} + x} \sqrt[4]{bx + 1} \left( A {}_2F_1 \left( \frac{\sqrt{a(10a - b)} - 3a}{2a}, -\frac{3a + \sqrt{a(10a - b)}}{2a}; \frac{1}{2}; -\frac{axb + b}{a - b} \right) \right)$$

$$\begin{aligned}
& +B\sqrt{\frac{b(ax+1)}{a-b}} {}_2F_1\left(-\frac{2a+\sqrt{a(10a-b)}}{2a}, \frac{\sqrt{a(10a-b)}}{2a}-1; \frac{3}{2}; -\frac{axb+b}{a-b}\right) \\
& / \left(\sqrt[4]{ax+1}\sqrt[4]{\frac{1}{b}+x}\right) \tag{5.19}
\end{aligned}$$

which are still in terms of hypergeometric functions.

The form of hypergeometric functions in (5.19) suggest that relating the Vaidya–Tikekar coefficients  $a$  and  $b$  by  $b = a(10 - k^2)$  for some natural number  $k$ , may yield solutions in elementary functions. For this choice the general solution is given by

$$\begin{aligned}
y & = a(k^2 - 10) \sqrt[4]{\frac{1}{a} + x} \sqrt[4]{a(k^2 - 10)x - 1} \\
& \left( A {}_2F_1\left(\frac{1}{2}(-k-3), \frac{k-3}{2}; \frac{1}{2}; \frac{(k^2-10)(ax+1)}{k^2-9}\right) \right. \\
& \left. + B\sqrt{\frac{(k^2-10)(ax+1)}{9-k^2}} {}_2F_1\left(-\frac{k}{2}-1, \frac{k-2}{2}; \frac{3}{2}; \frac{(k^2-10)(ax+1)}{k^2-9}\right) \right) \\
& / \left( \sqrt[4]{ax+1} \sqrt[4]{\frac{1}{10a-ak^2} + x} \right) \tag{5.20}
\end{aligned}$$

still containing the hypergeometric functions. Consider some special cases. For  $k = 1$  we get

$$\begin{aligned}
y & = \left( aA(9ax+11) + c_2(9ax+61)\sqrt{ax+1}\sqrt{9ax+1} \right. \\
& \left. - 8B(9ax+11) \log\left(-9ax-3\sqrt{ax+1}\sqrt{9ax+1}-5\right) \right) / a \tag{5.21}
\end{aligned}$$

For  $k = 2$  we get

$$\begin{aligned}
y & = \sqrt[4]{6ax+1} \left( -72a^2Bx^2\sqrt{-6ax-1} + 126aBx\sqrt{-6ax-1} - 4aA\sqrt{ax+1} \right. \\
& \left. + 398B\sqrt{-6ax-1} + 375B\sqrt{6ax+6} \sin^{-1}\left(\sqrt{\frac{6}{5}}\sqrt{ax+1}\right) \right)
\end{aligned}$$

$$/ \left( 4a\sqrt[4]{-6ax-1} \right) \quad (5.22)$$

For  $k = 4$  we get

$$y = A(1-6ax)^{7/2} - \frac{2B\sqrt{ax+1}(3456a^3x^3 - 3744a^2x^2 + 2724ax - 2081)}{84035a} \quad (5.23)$$

and so forth. The parameter  $k$  must be greater than or equal to  $\frac{1}{2}$  and must not be equal to 3. In this way we are able to generate a large class of exact solutions for third order Lovelock gravity in 8 dimensions.

More generally inserting  $b = 10a$  in equation (5.20) we get

$$y = - \left( \sqrt[4]{10ax+1} \left( 3\sqrt{10}B(20a^2x^2 + 67ax + 47) \sin^{-1} \left( \frac{1}{3}\sqrt{-10ax-1} \right) + 2(60a^3Ax^2 + 201a^2Ax - 55aBx\sqrt{-10ax-1}\sqrt{ax+1} - 73B\sqrt{-10ax-1}\sqrt{ax+1} + 141aA) \right) \right) / \left( 6a\sqrt[4]{-10ax-1}\sqrt{ax+1} \right) \quad (5.24)$$

as an exact solution. Therefore equation (5.20) admits a large variety of exact solutions expressible as elementary functions. In forthcoming work, we shall study the properties of such solutions more intensively.

## 5.4 Conclusion

We studied the most general Lovelock polynomials for all  $N$  and  $d$  values but for the critical spacetime dimensions  $d = 2N + 1$  and  $d = 2N + 2$ . We specialized to the cases  $N = 3$ ,  $d = 7$  and  $d = 8$  which have not been studied before. We considered the Vaidya-Tikekar metric potential and found solutions as hypergeometric functions. The form of hypergeometric functions in the Vaidya-Tikekar ansatz suggested that

relating the coefficients  $a$  and  $b$  by  $b = a(10 - k^2)$  for some natural number  $k$ , yields solutions in the elementary functions. We then considered some special cases which admitted a large variety of exact solutions expressible as elementary functions;  $k = 1, 2, 4$  and so forth where  $k \geq \frac{1}{2}$  and  $k \neq 3$ . Other potentials were also considered; the Schwarzschild interior metric and the Finch–Skea metric. A full physical analysis of solutions was not conducted since it would lie outside the scope of our thesis.

# Chapter 6

## Conclusion

The aim of this thesis was to investigate the behaviour of some well known general relativity models in higher curvature gravity. It was to generate their higher curvature counterparts in Lovelock gravity and then to study the effect of the higher order properties on the gravitational behaviour of perfect fluids.

We now provide an overview of the principal results obtained during the course of our analysis.

In chapter 3 we examined the specific case  $N = 2$ ,  $d = 5$  that enabled us to integrate the pressure isotropy condition and we found new five dimensional solutions to the  $5D$  pure Gauss–Bonnet field equations. We considered some special cases of physically important metric potentials to find these solutions. We began by considering the generalisation of the Vaidya–Tikekar ansatz since this choice is known to be useful in developing models of superdense stars in standard Einstein theory. We then analysed special cases of the Vaidya–Tikekar potential such as inserting  $b = 0$  and  $a = 1$  in the Vaidya–Tikekar ansatz to give the interior Schwarzschild solution;  $b = 1$  and  $a = 0$  resulted in the  $5D$  Finch–Skea model;  $b = 0$  and  $a = 0$  generated a version of the constant potential isothermal fluid. The physical properties of these

metrics in this chapter fulfilled our expectations as most of our graphical plots were physically pleasing. It was already well known that in  $d = 2N + 1$  no bounded distribution exist which means that the pressure cannot vanish at any finite radius. We were able to deduce this from the field equations directly.

In chapter 4 we analysed the six dimensional pure Gauss–Bonnet gravity ( $d = 2N + 2$ , where  $N = 2$ ). We implemented the same procedures used in the previous chapter to find solutions for this chapter. We again used the Vaidya–Tikekar potential as a prime case, but it was established that in  $6D$ , the general Vaidya–Tikekar metric gave rise to hypergeometric solutions. New special cases that reduce hypergeometric functions to elementary functions were found. We also examined other special cases like the existence of conformal killing vectors, the inverse square law fall–off of the temporal potential but was unable to proceed with the detailed physical analysis since we found implicit solutions in these cases. A handbook of exact solutions for ordinary differential equations [35] was used to implement a sequence of transformations to cast a nonlinear first order differential equation in the standard Abelian form. We then found exact solutions for these but they were expressible in implicit form. Therefore we were unable to study these models further since we did not have an explicit solution. Our main result was that in  $6D$  it was established that spacetimes do admit surfaces of vanishing pressure unlike in  $5D$ . We show this is true since it is possible to have  $p(R) = 0$  for large range of  $Z$  and  $y$  functions. We also realise that while most published works have carefully studied Einstein–Gauss–Bonnet effects in  $5D$ , there are generic problems. Our belief is that the  $6D$  case is of greater physical importance and is worthy of more extensive study.

In chapter 5 we examined the general Lovelock polynomials for all  $N$  and  $d$  values for the critical spacetime dimensions ( $d = 2N + 1$  and  $d = 2N + 2$ ), but specialised to the cases  $N = 3$ ,  $d = 7$  and  $d = 8$ . We again implemented the same procedures used in previous chapters. A large variety of exact solutions were found. The physical

conditions of the general Lovelock equations were examined but a thorough treatment was not done on this case since it lies outside the thesis purpose. This will be a matter of future research. While the cubic Lovelock term does not have a clear physical motivation as the quadratic Gauss–Bonnet term, it will be interesting to analyse further how higher curvature effect influence the formation and evolution of stars.

We have shown that higher curvature effects have a strong influence on models of static stars. In future work we shall examine more thoroughly the boundary conditions involved. We will match the interior and exterior solutions, and be able to find masses and radii for our choice of parameters. Alternatively, using the mass and radius of known stars we can fix the constants of integration in our models. Studying the behaviour of our models in the area of observational astrophysics will be an exciting future project.

# Bibliography

- [1] B. Cvetković and D Simić, *Phys. Rev. D* **94** , 084037 (2016); arXiv:1608.07976
- [2] T. Padmanabhan, *Gravitation: Foundations and Frontiers*. Cambridge University Press, Cambridge, UK, 2010
- [3] S. M. Carroll, *Lecture notes on general relativity*, arXiv:gr-qc/9712019
- [4] K. Parattu, S. Chakraborty, B. R. Majhi and T. Padmanabhan, *Gen. Rel. Grav.* **48** no. 7, (2016); arXiv:1501.01053
- [5] D. Lovelock *J. Math. Phys.* **12** 498 (1971)
- [6] G. W. Horndeski, *Int. J. Theor. Phys.* **10**, 363-384; (1974)
- [7] N. Dadhich, *Relativity and Gravitation: 100 Years after Einstein*, Prague eds. J Bicak, T Ledvinka (Springer, 2013); arxiv:1210.3022
- [8] N. Dadhich, S. G. Ghosh and S. Jhingan, *Physical Review D* **88**, 084024 (2013); arXiv:1308.4312
- [9] S. Chakraborty and N. Dadhich, *Eur. Phys. J. C* **78**, 81 (2018); arXiv:1605.01961
- [10] M. A. H. MacCallum, *Exact solutions of Einstein's equations*. Scholarpedia, **8** (12) : 8584 (2013)

- [11] H. Stephani, D. Kramer, M. A. H. MacCallum, C. Hoenselaers and E. Herlt, *Exact Solutions of Einstein's Field Equations*, 2nd Edition, Cambridge University Press (2003)
- [12] F. Canfora, A. Giacomini and S. A. Pavluchenko, *General Relativity and Gravitation* **46**, 1805 (2014); arXiv:1409.2637
- [13] S. Hansraj, B. Chilambwe and S. D. Maharaj, *Eur. Phys. J. C* **27** 277 (2015)
- [14] S. D. Maharaj, B. Chilambwe and S. Hansraj, *Phys. Rev. D* **91**, 084049 (2015)
- [15] B. Chilambwe, S. Hansraj and S. D. Maharaj, *Int. J. Mod. Phys. D* **24** 1550051 (2015)
- [16] H. Maeda and N. Dadhich, *Phys. Rev. D* **75**, 044007 (2007)
- [17] X. O. Camanho and N. Dadhich, *The European Physical Journal C* **76**, 3 (2016)
- [18] N. Dadhich, *Pramana* **74**, 875 (2010); arxiv:0802.3034
- [19] S. Hansraj and B. Chilambwe, *Eur. Phys. J. Plus* **19** 130 (2015)
- [20] P. C. Vaidya and R. Tikekar, *J. Astrophys.* **3** 325 (1982)
- [21] N. Dadhich, A. Molina and A. Khugaev, *Phys. Rev.* **81**, 104026 (2010); arxiv:1001.3952
- [22] W. C. Saslaw, S. Maharaj and N. Dadhich, *Astrophys. J.* **471**, 571 (1996)
- [23] N. Dadhich, S. Hansraj and S. D. Maharaj, *Phys. Rev. D* **93** 044072 (2016)
- [24] M. D. Roberts, *II Nuovo Cimento B* **110**,10 (1995)
- [25] S. Chandrasekhar, *Astrophys.J.* **140**, 417 (1964)
- [26] S. Chandrasekhar, *Phys. Rev. Lett.* **12**, 114 (1964)

- [27] M. R. Finch and J. E. F. Skea, *Class. Quant. Grav.* **6** 467 (1989)
- [28] N. Dadhich, A. Molina and A. Khugaev, *Phys. Rev. D* **81**, 104026 (2010)
- [29] S. Hansraj, *Euro. Phys. J. C* **77**, 8 (2017)
- [30] F. Rahaman, S. Mal and M. Kalam, *Vacuumless topological defects in Lyra geometry, Astrophys Space Sci.* **319**, 169-175 (2009).
- [31] P. C. Vaidya and R. Tikekar, *J. Astrophys.* **3**, 325 (1982)
- [32] H. Knutsen, *Astrophys. Space Science* **98**, 207 (1984)
- [33] H. A. Buchdahl, *Phys. Rev.* **116**, 1027 (1959)
- [34] H. A. Buchdahl, *Class. Quantum. Grav.* **1**, 301 (1984)
- [35] A. D. Polyanin and V F Zaitsev, *Handbook of Exact Solutions for Ordinary Differential Equations.* CRC Press (1995)